Experimental and theoretical studies of quadrupolar oligothiophene-cored chromophores containing dimesitylboryl moieties as π-accepting end-groups: Syntheses, structures, fluorescence, one- and two-photon absorption

Lei Ji,[a,b] Robert M. Edkins,[a,b] Laura J. Sewell,[a] Andrew Beeby,[a] Andrei S. Batsanov,[a] Katharina Fucke,[b,c] Martin Drafz,[a] Judith A. K. Howard,[a] Odile Moutounet,[d] Fatima Ibersiene,[d] Abdou Boucekkine,[d] Eric Furet,[d] Zhiqiang Liu,[a,e] Jean-François Halet,*[d] Claudine Katan,*[d,f] Todd B. Marder*[a,b]

[a] Dr. L. Ji, Dr. R. M. Edkins, Dr. L. J. Sewell, Prof. Dr. A. Beeby, Dr. A. S. Batsanov, M. Drafz, Prof. Dr. J. A. K. Howard, Prof. Dr. Z. Liu, Prof. Dr. T. B. Marder

Department of Chemistry, University of Durham, South Road, Durham, DH1 3LE, UK.

[b] Dr. L. Ji, Dr. R. M. Edkins, Dr. K. Fucke, Prof. Dr. T. B. Marder

Institut für Anorganische Chemie, Julius-Maximilians-Universität Würzburg, Am Hubland, 97074 Würzburg, Germany. Email: todd.marder@uni-wuerzburg.de

[c] Dr. K. Fucke

School of Medicine, Pharmacy and Health, Durham University, University Boulevard, Stockton-on-Tees, TS17 6BH, UK

[d] O. Moutounet, Dr. F. Ibersiene, Prof. Dr. A. Boucekkine, Dr. E. Furet, Prof. Dr. J. -F. Halet, Dr. C. Katan

Institut des Sciences Chimiques de Rennes, UMR 6226, CNRS, Université de Rennes 1, Ecole Nationale de Chimie de Rennes, 35042 Rennes, France. Email: jean-francois.halet@univ-rennes1.fr, claudine.katan@univ-rennes1.fr

[e] Prof. Dr. Z. Liu

State Key Laboratory of Crystal Materials, Institute of Crystal Materials, Shandong University, Jinan 250100, PR China.

[f] Dr. C. Katan

Université Européenne de Bretagne, FOTON, UMR 6082 CNRS-INSA de Rennes, F-35708 Rennes, France.

Abstract

Quadrupolar oligothiophene chromophores composed of four to five thiophene rings with two terminal (*E*)-dimesitylborylvinyl groups (**4V**-**5V**), and five thiophene rings with two terminal aryldimesitylboryl groups (**5B**), as well as an analogue of **5V** with a central EDOT ring (**5VE**), have been synthesized *via* Pd-catalyzed cross-coupling reactions in high yields (66-89%). Crystal structures of **4V**, **5B**, bithiophene **2V**, and five thiophene-derived intermediates are reported. Chromophores **4V**, **5V**, **5B** and **5VE** have photoluminescence quantum yields of 0.26-0.29, which are higher than those of the shorter analogues **1V**-**3V** (0.01-0.20), and short fluorescence lifetimes (0.50-1.05 ns). Two-photon absorption (TPA) spectra have been measured for **2V**-**5V**, **5B** and **5VE** in the range 750-920 nm. The measured TPA cross-sections for the series **2V**-**5V** increase steadily with length up to a maximum of 1930 GM. We compare the TPA properties of **2V**-**5V** with the related compounds **5B** and **5VE**, giving insight into the structure-property relationship for this class of chromophore. DFT and TD-DFT results, including calculated TPA spectra, complement the experimental findings and contribute to their interpretation. A comparison to other related thiophene and dimesitylboryl compounds indicates that our design strategy is promising for the synthesis of efficient dyes for two-photon-excited fluorescence applications.

Introduction

Over the past decade, two-photon absorption (TPA) has attracted a tremendous research effort, especially from synthetic chemists in the quest of designing new chromophores that combine enhanced TPA responses and appropriate properties for particular applications. The latter range from materials science to medicine and have prompted a series of review papers in recent years addressing TPA fundamentals, scope in terms of applications, as well as various synthetic strategies implemented for the design of TPA chromophores.[1] Among the benefits of TPA over alternative techniques, spatiotemporal control of excitation and/or fluorescence is probably the most prominent. It is a direct byproduct of the simultaneous absorption of a pair of photons that may have different or the same energies. Such fine spatiotemporal control, combined with the use of near-IR excitation, meets the prerequisites for photochemical tools capable of investigating the dynamics of biological processes. Indeed, several recent reviews demonstrate both achievements and needs of sensing, imaging, and

uncaging carried out within living cells and tissues or applied to the study of physiological processes.[2]

At the same time, boron chemistry has expanded its use from material to medical science where it is believed to provide a new class of molecules for imaging or therapeutic agents.[3] Boron chemistry has also contributed to a major advance in the field of molecular machines, with the discovery of a double stranded helicate bridged by two spiroborate moieties capable of undergoing a reversible spring-like motion triggered by inclusion and removal of a sodium ion.[4] Unlike four-coordinated boron, three-coordinated boron can be incorporated in π-conjugated molecules where it usually acts as a π-acceptor due to its vacant p-orbital, while remaining a strong σ-donor.[5] To prevent attack of the three-coordinated boron center by nucleophiles, sterically-shielding substituents, such as mesityl (2,4,6-trimethylphenyl) groups, have proved efficient, limiting, at the same time, π-stacking in condensed phases.[6] This has opened the way for the design of conjugated boron-based chromophores with interesting linear and non-linear optical properties. However, despite numerous studies of the structure-property relationship for TPA response over more than a decade,[1] chromophores built from dimesitylboryl π-accepting moieties are still relatively rare [7-14] as are those containing oligothiophene moieties.[8,11,14-20]
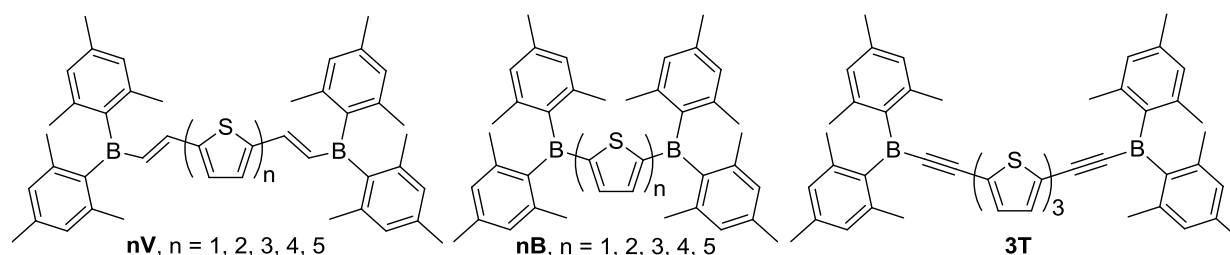
Scheme 1. Chromophores **1V**-**5V** (left), **1B**-**5B** (middle) and **3T** (right). Single-crystal X-ray diffraction data are available for compounds **1V**-**4V** and **5B**.
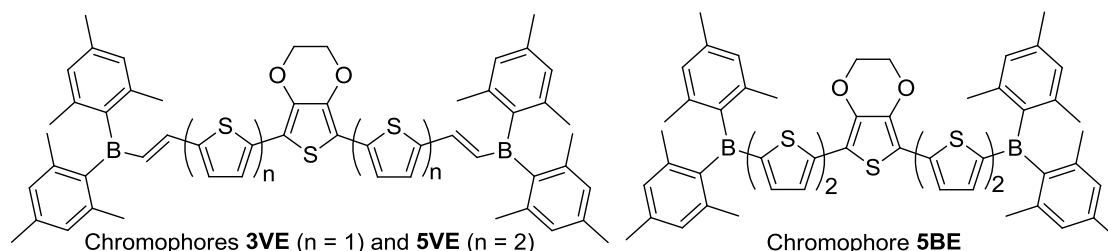
Scheme 2. Chromophores **3VE** and **5VE** (left) and **5BE** (right).

This prompted us to investigate further the TPA properties of A-D-A quadrupoles containing both of these electron accepting and donating building blocks, in line with the earlier work by some of us.[14] In fact, we have shown that symmetric (*E*)-dimesitylborylvinyl dithiophene (**2V**) and terthiophene (**3V**) (Scheme 1) have promising TPA cross-sections and clear TPA enhancement upon chain elongation with a concomitant two-fold increase of the radiative quantum yield. To investigate further the structure-property relationships of this class of chromophores, we report herein our investigations of both the chain length effect with **4V** and **5V** (Scheme 1) and the nature of the conjugated bridge by removing the vinylene spacers (**5B**, Scheme 1). Further diversification was also considered with the inclusion of the electron donating 3,4-ethylenedioxythiophene (EDOT) unit (**5VE**, Scheme 2), in a comparable strategy to the one recently developed for D-A-D conjugated oligomers.[15]

In the present paper, we present first the synthesis and characterization of the aforementioned compounds and then discuss their crystal structures and molecular geometries as derived from single-crystal X-ray diffraction data and density functional theory (DFT) optimized geometries, respectively. Theoretical calculations were used to extend the scope of the study by investigating all chromophores sketched in Schemes 1 and 2. Next, one-photon absorption (OPA), emission, solvatochromism and TPA are discussed in sequence, aided by TD-DFT calculations relevant for the ground state conformations and anterior few-state modeling for the emission properties.[21] Finally, the TPA activity of our quadrupolar chromophores is compared to that of related compounds built from either $BMes_2$[8-13] or oligothiophene moieties,[15-20] allowing additional insight into structure-TPA relationships.

Results and Discussion
Synthesis

The compounds were synthesized as summarized in Scheme 3. Compounds **2V** and **3V** were synthesized by direct hydroboration of the respective diterminal alkynes, according to the published procedure.[14]

In the synthesis of compound **4V**, using a similar procedure as for **2V** and **3V**, it proved difficult to isolate the intermediate dibromoquaterthiophene **2** because of its poor solubility. In the synthesis of **2V** and **3V**, we found that the compound 5,5''-diethynyl-2,2':5',2''-terthiophene tended to darken and become insoluble when it was heated to 40 °C under vacuum on a rotary evaporator. Therefore, the solvent must be removed on a vacuum line

4

without heating. The two pure diynes (5,5'-diethynyl-2,2'-bithiophene and 5,5''-diethynyl-2,2':5',2''-terthiophene) turn dark and become insoluble after storage for two weeks. This may be caused by polymerization, which occurs slowly at room temperature and very fast when heated, even under vacuum. Therefore, even if we were able to isolate **2** to prepare 5,5'''-diethynyl-2,2':5',2'':5'',2'''-quaterthiophene, the latter is not predicted to be a very stable compound according to the trend observed for its di- and terthiophene analogues. Instead, we prepared the bis(boronate) **2Bpin** *via* Ir-catalyzed C–H borylation[22] of dithiophene **5**. Suzuki-Miyaura coupling of compound **4** and **2Bpin** using $K_3PO_4 \cdot H_2O$ as base and Pd(dppf)Cl$_2$ as catalyst at 90 °C in DMF was attempted to synthesize **4V**. However, none of the target compound was isolated, whereas **4** was fully consumed according to TLC analysis, even when it was used in excess. It has been reported by Wang and co-workers[23] that some ArylBMes$_2$ compounds can act as mesityl transfer agents in Suzuki-Miyaura coupling reactions under certain conditions. ArylBMes$_2$ compounds are stable in Sonogashira and Heck reactions when using amine bases,[12] so it is likely that only small basic groups such as fluoride and hydroxide ion can attack the bulky boron center causing problems in palladium-catalyzed reactions. It is also possible that some protodeborylation of **2Bpin** occurred under our reaction conditions. With these issues in mind, we then employed a Stille coupling reaction, which does not require added base.

Coupling of **4** with **2Sn**, using Pd(PPh$_3$)$_4$ as the catalyst in DMF at 90 °C, resulted in a high yield (89%) of **4V**. Compounds **5V**, **5VE**, and **5B** were synthesized using similar reaction conditions, all with high yields (66-89%). Compound **5B** was also synthesized by Suzuki-Miyaura coupling of **8** with **3Br** in a comparable yield (88%), which suggests that ArylBMes$_2$ is a more stable group than vinylBMes$_2$ in Suzuki-Miyaura couplings and that, contrary to our initial concern, thiophene-BMes$_2$ groups do not necessarily undergo mesityl transfer under Suzuki-Miyaura coupling reaction conditions.

To synthesize compound **13**, Suzuki-Miyaura coupling of **6** and **12** using Pd(dppf)Cl$_2$ as the catalyst and $K_3PO_4 \cdot H_2O$ as the base, was initially attempted. However, compound **12** undergoes protodeborylation and polymerization, so we did not obtain **13** *via* this reaction. Thus, **13** was synthesized *via* Suzuki-Miyaura coupling of **14** with 2-(Bpin)thiophene.
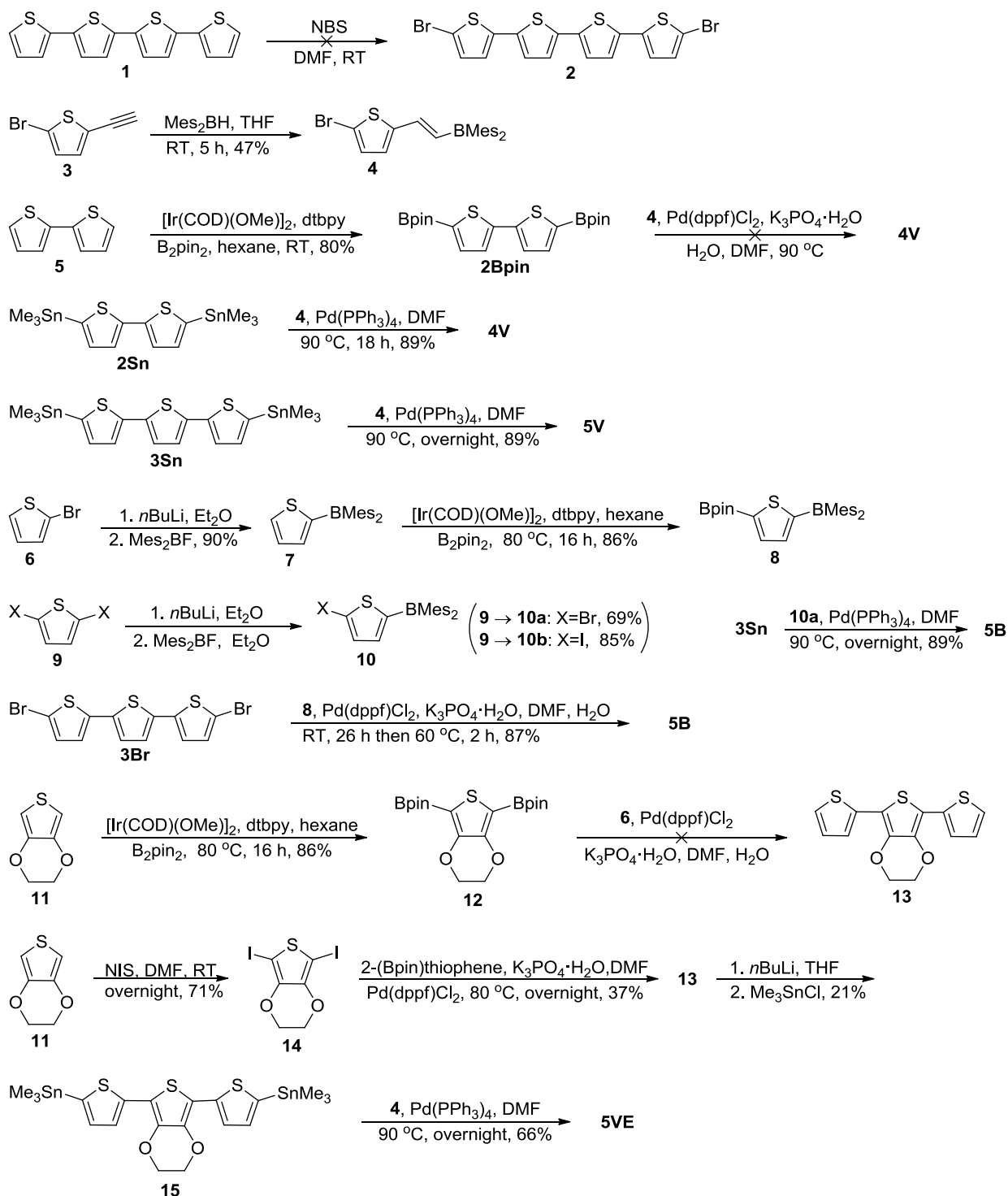
Scheme 3. Synthesis of **4V**, **5V**, **5B**, and **5VE**.

Crystal structures and molecular geometries

Structural information has been derived both from single-crystal X-ray diffraction data and calculated optimized geometries in vacuum (experimental section). Although they belong to two extremes regarding the nature and strength of chromophore interactions with their

surroundings, both provide information about the structure-property relationships of the investigated compounds. The molecular structures of compounds **1V** and **3V** have been published previously,[14] and we report herein the structures of **2V**, **4V** and the toluene hemisolvate of **5B** (Figure 1). Crystals of **2V** were obtained from hexane, while those of **4V** and **5B** were grown by slow diffusion of methanol into toluene solutions. All bond lengths are in the normal ranges.[24] In addition, the crystal structures of synthetic intermediates **4**, **7**, **8**, **10b**, and **12** have been determined (see ESI Figures S1-S5). Crystallographic data of all compounds are listed in Tables S1-S3, while Table 1 summarizes corresponding intramolecular torsional angles and bond lengths, including crystallographic data previously reported for **1V** and **3V** for comparison.[14] Similar data for **4**, **7**, **8**, **10b**, and **12** are presented in Table S4.
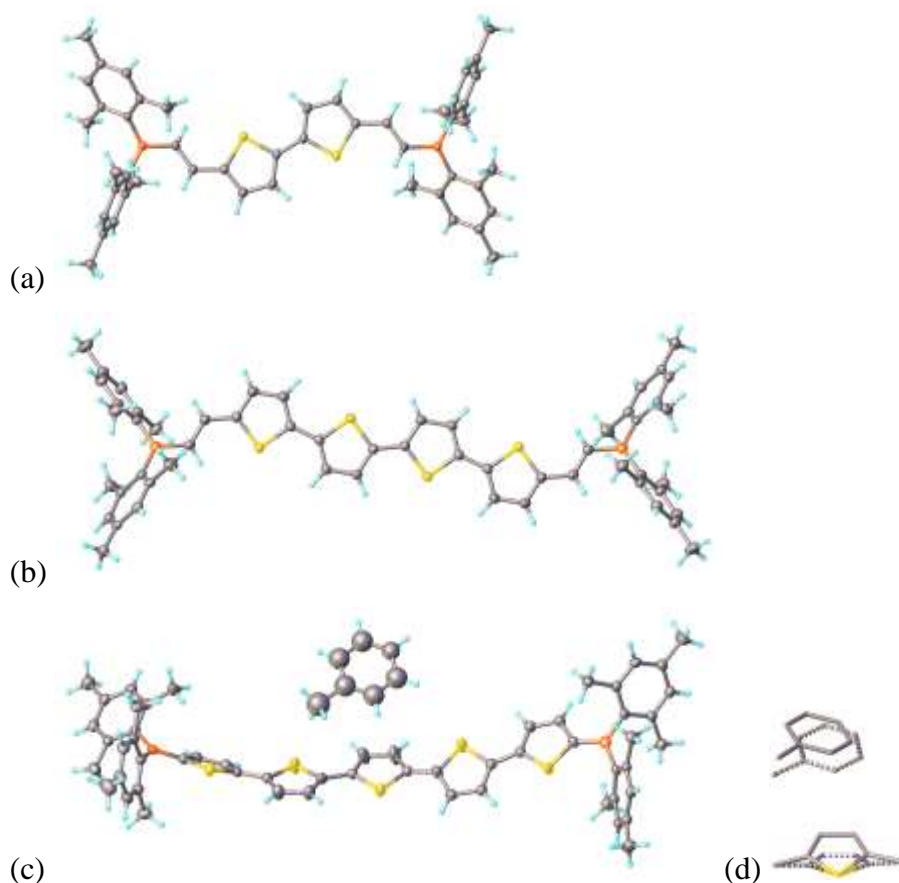

(a)

(b)

(c)   (d)

Figure 1. Molecular structures of compounds **2V** (a), **4V** (b) and **5B**·½PhMe (c), and disordered toluene and central thiophene ring fragments of the latter (d), from single-crystal X-ray diffraction. Atomic displacement ellipsoids are drawn at 50% probability level. Element (color): carbon (gray), hydrogen (pale blue), sulfur (yellow) and boron (orange).

All new crystal structures containing more than one thiophene ring reveal an *all-trans* conformation, *i.e.* with S atoms pointing in opposite directions. B3LYP/6-31G* optimized geometries support the preference for this conformation and suggest possible coexistence of both *trans* and *cis* conformers in solution at room temperature (RT) only for the compounds with the lowest number of thiophene rings. Concerning the vinyl-containing compounds, both *cisoid* and *transoid* conformers are experimentally evidenced with a preference for the *transoid* conformation when the molecule can adopt C_i symmetry, *i.e.* for an even number of thiophene rings. However, we reported previously that the crystal structure of **1V** contains two symmetrically independent molecules realizing both *cisoid* and *transoid* conformers.[14] In addition, calculations show that both conformers are energetically close enough to be present in solution at RT.

The crystal structures (Table 1) generally confirm the theoretical predictions. Crystals of **2V** and **4V** do not incorporate solvent; in both, the molecule has a crystallographic inversion center and the oligothiophene is practically planar, maximizing conjugation along the backbone. In addition, there is no twist between the terminal thiophene rings (measured as the torsion angle). On the contrary, all three compounds with an odd number of thiophene rings crystallize as solvates. The oligothiophene systems in **3V** and **5B** are substantially arched, as well as twisted, and have no crystallographic symmetry. Such bent conformations and the incorporation of solvent are likely interrelated factors, which should be taken into account when comparing the gas phase, solid state and solution structures. However, both the bending and twisting of the oligothiophene moieties are noticeable in the DFT gas-phase calculations of **3V** and **5V** (Figure S6), indicating that these are inherent properties of the molecules. The central thiophene ring of **5B** exhibits flipping disorder, modeled over two positions with 50% occupancy each, which is correlated with the disorder of an adjacent toluene molecule over two positions related *via* a crystallographic twofold axis.

As reported for related structures,[5e, 5k, 25] the mesityl rings attached to the boron core orient in a propeller-like fashion with a trigonal planar geometry around the boron atom. Thus, conjugation between the boron atom and the mesityl groups is limited, and electron deficiency on the boron atom is maintained. The addition of a vinyl spacer between the BMes$_2$ groups and the thiophene backbone introduces a dihedral angle of up to 30º between the oligothiophene-divinyl backbone and the trigonal plane of the boron-containing group, independent of solvate formation. In **5B**, the B-bonded thiophene moiety is rotated out of the BC$_3$ plane by only 10.6(1)°. Even though no crystal structures could be obtained to confirm

this finding, no perceptible change in the molecular geometry is predicted by DFT optimizations when the central thiophene ring is substituted by an EDOT moiety.

Table 1. Selected structural data from the crystal structures of **1V**-**4V** and **5B**. M1, M2, M3 and M4 are planes of mesityl substituents of the terminal $BMes_2$ groups; $\tau = |180° -$ torsion angle B-C=C-C(thiophene)|; V = vinyl moiety B-C=C-C(thiophene); $\theta =$ torsion angle between terminal thiophene rings.

	$1V \cdot CH_2Cl_2$ [14]		2V	$3V \cdot CH_2Cl_2$ [14]	4V	$5B \cdot \frac{1}{2}PhMe$
$B1C_3$/M1 [°]	63.61(8)	48.36(8)	64.15(5)	59.16(8)	56.24(8)	60.1(1)
$B1C_3$/M2 [°]	52.15(9)	62.05(8)	49.48(5)	42.52(8)	60.15(9)	55.0(1)
$B1C_3$/V [°]	14.6(2)	24.6(2)	22.3(1)	28.8(2)	19.4(2)	
$B1C_3$/thio1 [°]						10.6(1)
$B2C_3$/M3 [°]	47.71(8)	60.97(8)		58.45(9)		57.3(1)
$B2C_3$/M4 [°]	51.73(8)	57.01(9)		53.65(9)		62.6(1)
$B2C_3$/V [°]	30.0(2)	15.1(2)		23.1(2)		
V/thio1 [°]	7.6(2)/	19.8(2)/	16.4(1)	12.5(2)/	7.9(2)	
	10.2(2)	1.1(2)		3.8(2)		
thio1/thio2 [°]			0	10.95(8)	2.54(8)	7.8(1)
thio2/thio3 [°]				6.21(8)	0	A 23.2(2)
						B 7.7(3)
thio3/thio4 [°]						A 9.9(2)
						B 35.3(2)
thio4/thio5 [°]						25.4(1)
$B2C_3$/thio5 [°]						17.9(1)
τ [°]	τ_1 3.1	τ_1 7.4	13.8	τ_1 5.1	5.75	τ_1 3.98
	τ_2 0.8	τ_2 4.2		τ_2 6.6		τ_2 5.58
θ [°]			0	15.4	0	30.6
thio1/thio3 [°]				15.36(8)		
thio1/thio5 [°]						54.68(9)
B-C(Mes) [Å]	1.577(4)	1.575(4)	1.578(2)	1.574(3)	1.580(3)	1.578(4)
B-C(non-Mes) [Å]	1.552(3)	1.552(3)	1.550(2)	1.556(3)	1.548(3)	1.543(5)

In addition to the comparison between molecular geometries derived from X-ray data and those optimized in vacuum, the bond length alternation (BLA) of carbon-carbon bonds is often used to correlate structural data with NLO properties.[26] It is generally believed that the lower the BLA value, the higher the degree of conjugation, which, in turn, is beneficial for

increasing the hyperpolarizability of the molecule. Available data are summarized in Tables 2 and S5. The BLA values from DFT calculations show a slight but significant decrease for the series **1V**-**5V**, *i.e.* with an increase in the number of thiophene rings, while it slightly increases for the series **1B**-**5B**. This is a direct consequence of the absence or presence of the vinylene spacers that have a large BLA. Thus, from the BLA values of the series **1B**-**5B**, one would expect reduced conjugation and less NLO enhancement when increasing the number of thiophene rings, as compared to series **1V**-**5V**. Although of high quality, the accuracy of the X-ray crystallographic data does not allow experimental confirmation of these trends.

Table 2. Single-crystal X-ray diffraction experimental and DFT-calculated (B3LYP/6-31G*) carbon-carbon bond length alternation (BLA [Å]).[a]

	Solid state (X-ray structure)	Vacuum (DFT)
1V	0.081/0.077[b]	0.059
2V	0.063	0.053
3V	0.073[b]	0.050
4V	0.068	0.048
5V		0.047
1B		0.016
2B	0.032[c]	0.033
3B		0.037
4B		0.038
5B	0.05/0.06[d]	0.039
3VE		0.047
5VE		0.046

[a] BLA values were calculated by subtracting the average length of all of the formally double C=C bonds from the average length of all of the formally single C–C bonds between the two boron atoms.
[b] Ref. [14].
[c] Containing $B(C_6F_5)_2$ groups replacing $BMes_2$.[27]
[d] Disordered molecular structure.

One-Photon Absorption (OPA)

All chromophores of series **1V**-**5V** and **1B**-**5B** show an intense absorption band in the blue-green region of the visible spectrum, and a bathochromic shift upon increasing the number of thiophene rings in the molecular backbone is observed (Figures 2 and 3; Tables 3 and 4). This red shift is accompanied by a hyperchromic effect, *i.e.* an increase in oscillator strength (Figure 3; Table 4), which is related to the nature of the underlying electronic redistribution

upon excitation. Natural transition orbitals[28] (NTOs) associated with the vertical transition between the ground state and the lowest excited state are shown for compounds **4B** and **4V** in Figure 4, and are provided in the Supporting Information for all other compounds (Figure S7). They show a close match with the frontier orbitals, and reveal delocalization over the whole molecular backbone of both the holes and the electrons, leading to an increase of transition dipole moments with elongation. The calculated systematic and comparable hyperchromic effect upon elongation for both the **1B**-**5B** and **1V**-**5V** series contrasts with the respective increase and decrease of their BLA (Table 2).
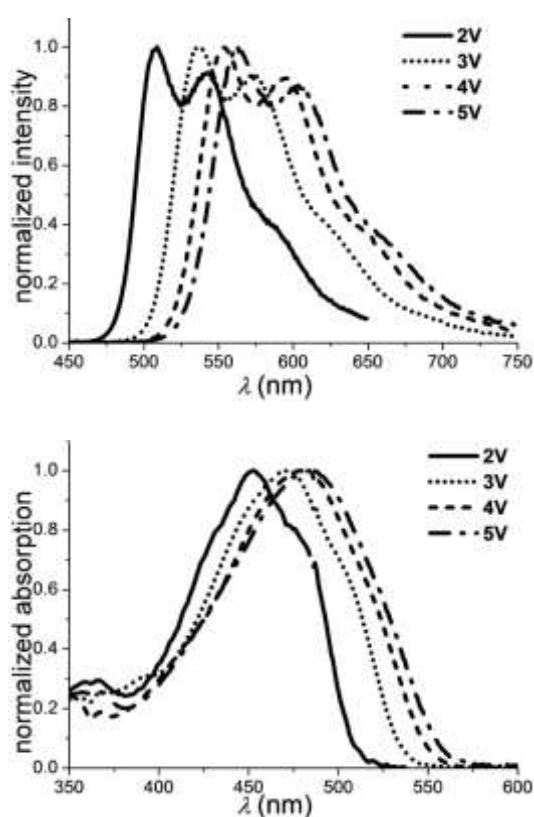
Figure 2. Normalized absorption (upper) and emission (lower) spectra of compounds **2V**-**5V** in toluene.
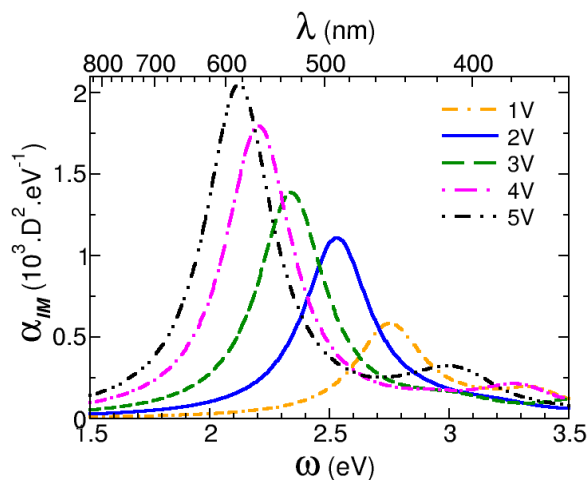
Figure 3. Calculated absorption spectra of compounds **1V**-**5V** in vacuum (TD-DFT B3LYP/6-31G*).

Table 3. Photophysical data for chromophores **2V**-**5V**, **5B**, and **5VE** in toluene, and available photophysical data for **1B**-**3B** from the literature.

	λ_{max}[abs] (nm)	ε (M^{-1} cm^{-1})	λ_{max}[em] (nm)	Stokes shift (cm^{-1})	Φ_f	τ_f (ns)	τ_0 (ns)	k_r (10^8 s^{-1})	k_{nr} (10^8 s^{-1})
1V[a]	411	48 000	452	2200	0.01	0.53	53	0.19	18.7
2V	453	52 000	509	2400	0.11	0.50	4.5	2.2	17.8
3V	470	57 000	536	2600	0.20	0.79	4.0	2.5	10.2
4V	486	70 000	554	2500	0.29	1.05	3.6	2.8	6.7
5V	487	76 000	563	2800	0.26	0.93	3.6	2.8	8.0
5VE	511	100 000	586	2500	0.26	0.98	3.8	2.6	7.6
1B[b]			440						
2B[b]	402	54 000	440	2100	0.86				
3B[b]	437	60 000	488	2400					
5B	467	79 000	540	2900	0.26	0.85	3.3	3.0	8.8

[a] Ref. [14], in cyclohexane. [b]. Ref. [29f], in THF.

Table 4. Calculated photophysical properties in vacuum relevant for the first excited singlet state: vertical transition energy (ω_{01}), transition wavelength (λ_{01}) and oscillator strength (f_{01}).

	1V	**2V**	**3V**	**4V**	**5V**	**2B**	**3B**	**4B**	**5B**	**5BE**	**3VE**	**5VE**	**3T**
ω_{01} (eV)	2.75	2.52	2.34	2.21	2.12	2.90	2.64	2.42	2.30	2.22	2.28	2.05	2.37
λ_{01}(nm)	450	492	528	561	585	428	470	512	540	559	543	603	523
f_{01}	0.96	1.79	2.09	2.55	2.79	1.00	1.61	2.05	2.42	2.45	2.15	2.81	2.24
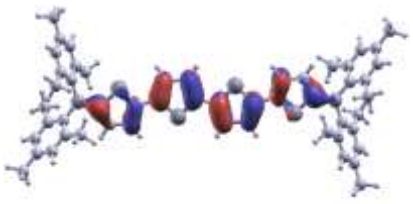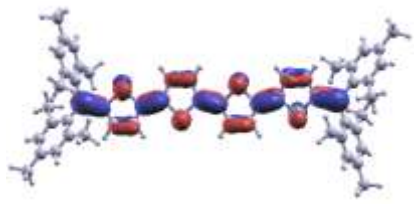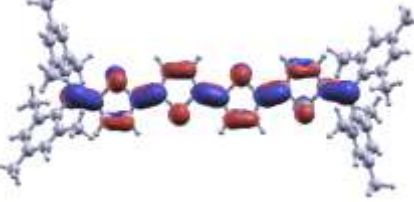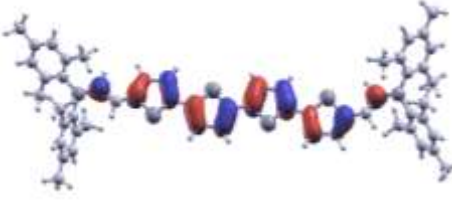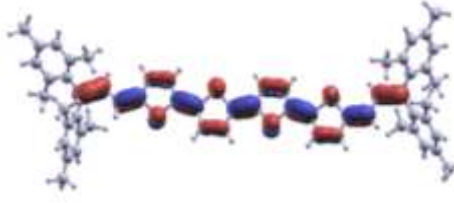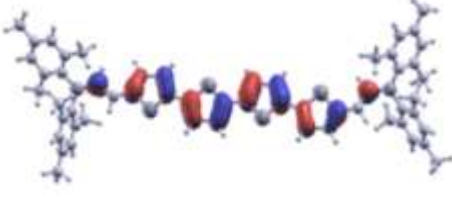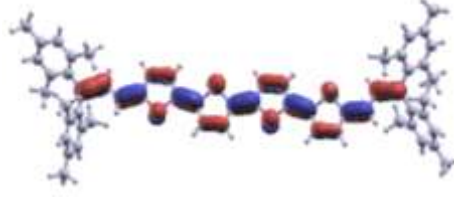
	Hole	*Electron*
NTO		
4B	*HOMO*	*LUMO*
MO		
	Hole	*Electron*
NTO		
4V	*HOMO*	*LUMO*
MO		

Figure 4. Natural transition orbitals (NTO: Hole/Electron) associated with the first excited state of chromophores **4B** and **4V** compared to frontier molecular orbitals (MO: HOMO/LUMO).

Chromophore **5B** shows a significant blue shift compared to its vinylene analogue **5V** (800 cm^{-1}, Table 3), leading to a normalized absorption band almost identical to that of **3V** (Figure 5). However, as indicated in Table 3, **5B** has a significantly larger molar extinction coefficient than **3V**, comparable to that of **5V** with the slight gain being compensated by a narrower bandwidth. These trends are confirmed by a theoretical investigation of the whole series **2B**-**5B** (Table 4, Figure S8). Thus, removal of the two vinylene spacers leads to blue-shifted bands of reduced oscillator strength; however, the larger the chromophore, the smaller

13

this effect becomes. Calculations show that replacement of the vinylene spacers of **3V** by ethynylene groups (**3T**) leads to a reduction in the blue shift of the absorption band and a slight oscillator strength enhancement (Table 4, Figure S9). Excited-state lifetimes were measured using the Time-Correlated Single-Photon Counting (TCSPC) technique. The data fit satisfactorily to a single exponential decay function in each case, with values in the range 0.50-1.05 ns (Table 3, Figure S10 for a representative example).
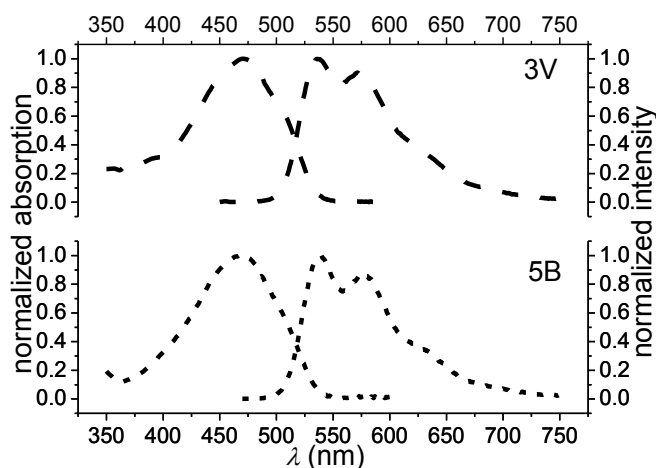

Figure 5. Normalized absorption and emission spectra of **3V** and **5B** in toluene.
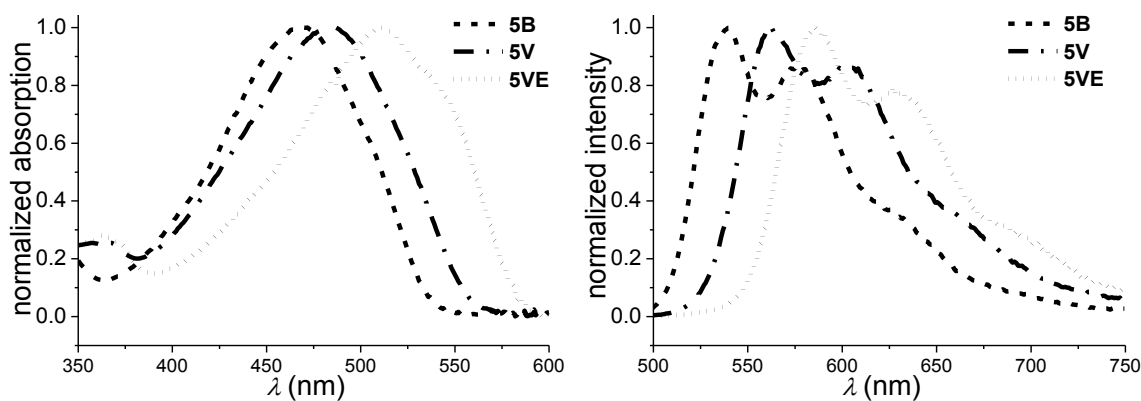

Figure 6. Normalized absorption (left) and emission (right) spectra of **5B**, **5V** and **5VE** in toluene.

Replacement of the central thiophene ring of **5V** by the electron-rich EDOT moiety (**5VE**) gives rise to a significant increase of the molar extinction coefficient (*ca.* 30%) and a further red shift of more than 700 cm^{-1} (Table 3, Figure 6). However, as a result of the narrower bandwidth, the oscillator strength shows little enhancement for the values calculated in vacuum (Table 4). Nevertheless, both the bathochromic shift and hyperchromic effect

introduced by the EDOT moiety are theoretically confirmed for compounds **3VE** and **5BE** (Table 4, Figures S8 and S9).
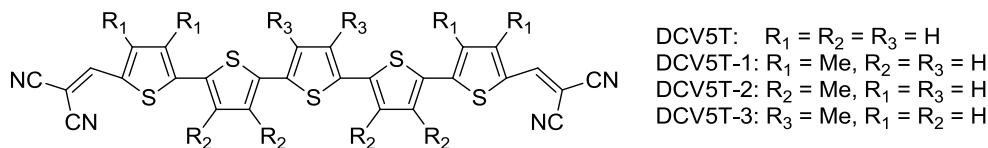
Scheme 4. Structure of DCV5T and its analogues.

The large molar extinction coefficients and broad absorption bandwidths of our compounds indicate their potential for application in organic solar cells. Indeed, Bäuerle and co-workers have recently reported dicyanovinyl-capped quinquethiophene (DCV5T) analogues (Scheme 4), whose structures are similar to our compounds **5V** and **5VE**, as donor materials for bulk heterojunction solar cells with high power conversion efficiencies (4.6-6.9%).[30] The shapes and positions of the absorption bands of the DCV5T analogues are almost the same as those of compound **5VE**, but **5VE** shows a larger molar extinction coefficient (10×10^4 M^{-1} cm^{-1}) than DCV5T (7×10^4 M^{-1} cm^{-1}).

Photoluminescence

Table 3 includes the photoluminescence data for all of the chromophores investigated experimentally. With the exception of **1V**,[14] all compounds exhibit moderate fluorescence quantum yields of 0.11-0.29 and sizeable Stokes shifts in toluene. The fluorescence can be tuned from deep green to red (Figure 7). Indeed, consistent with the red shift in absorption, increasing the oligothiophene length of the vinylene-based mesitylboryl compounds (**2V-5V**) induces a significant bathochromic shift in the emission of more than 1900 cm^{-1}. Replacement of the central thiophene ring by an EDOT moiety provides a further bathochromic shift, resulting in red emission (Figures 6 and 7), while maintaining a similar emission quantum yield (Table 3). Both **5B** and **5V** have the same quantum yield of 0.26, revealing that the incorporation of vinylene spacers does not influence this parameter. However, unlike the substitution by the EDOT ring, the absence of vinylene spacers does give rise to a noticeable hypsochromic shift, leading to overlapping emission spectra of **5B** with **3V**. A similar overlap is observed in the absorption spectra (Figure 5), *vide supra*. These findings, and theoretical predictions for the series **2B**-**5B** (Table 4), suggest that reducing the size of the oligothiophene unit offers a route to extend the emission range further to the blue end of the spectrum while maintaining sizeable radiative quantum yields.
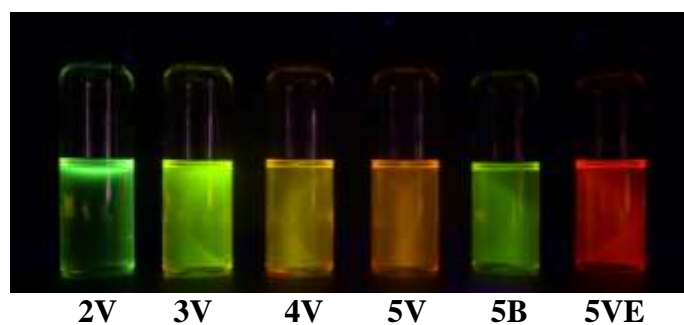
2V   3V   4V   5V   5B   5VE

Figure 7. Fluorescence of 10^{-5} M toluene solutions excited at 365 nm.

Solvatochromism

All of the new chromophores reported here exhibit a weak positive solvatochromic absorption behavior (Table S6). This behavior is similar to that previously reported for dipolar analogues,[5i,25e] and is consistent with earlier findings on **2V**, **3V** and other quadrupolar A-π-A systems containing π-accepting (*E*)-dimesitylborylvinyl groups.[14] These measurements reveal that the chromophores have non-polar ground states with small, if not vanishing, dipole moments as a result of an inversion center of symmetry in the molecules. In contrast, emission solvatochromism is much more pronounced (Table S6), suggesting polar emitting states as a consequence of significant reorganization of the excited state prior to emission.[21,31-32]

Such behavior has been reported for both quadrupolar and octupolar chromophores, and has been rationalized *via* the few-state model of Terenziani and co-workers.[21,31] These models predict unconditional symmetry breaking for octupolar dyes, so that excitation localization on a single branch occurs after excitation and prior to emission for any solvent, whereas the intramolecular charge transfer taking place upon excitation (absorption) is delocalized over the whole molecular backbone.[31] Lambert and co-workers have attributed this type of symmetry breaking in octupolar triarylboranes to the degeneracy of the exited state being lifted by a Jahn-Teller distortion.[32a] They also demonstrated that the excitation energy can be transferred among the three branches, which was rationalized by transition dipole-dipole interactions between chromophore subunits. Due to the unconditional nature of the multistability in the case of octupoles, such behavior is described well by state-of-the-art quantum mechanical approaches.[32b-d]
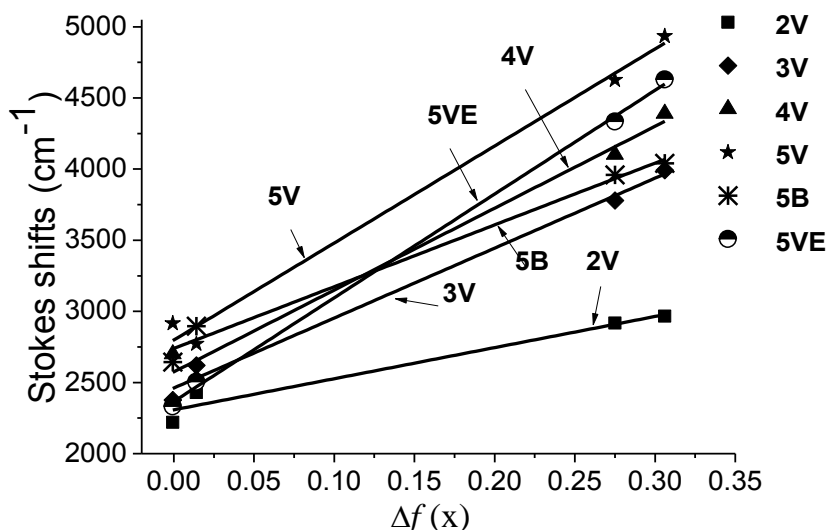
Figure 8. Lippert-Mataga plots for chromophores **2V**, **3V**, **4V**, **5V**, **5B**, **5VE**, using the standard definition of the orientation polarizability, Δf (x).[32d]

In contrast, quadrupolar chromophores may show distinctly different behavior depending on the nature of their charge distribution in the ground state and have been placed into three different classes.[21] Given that all quadrupoles of the present work show small and significant solvatochromic shifts in absorption and fluorescence, respectively, we assign them as belonging to Class I according to ref. [21]. For quadrupoles of this class, the potential energy surface relevant to the first excited state exhibits conditional bistability, with the possible appearance of two degenerate minima, corresponding to asymmetric deformations of the molecule that lead to a broken symmetry and localization of the excited state on either of two portions of the chromophore. This conditional bistability is related to the strength of electron-phonon coupling, and symmetry breaking is induced by relaxation of the solvation coordinate. At least in high polarity solvents, we expect our quadrupoles to undergo stabilization of the broken symmetry state, similar to that reported for fluorene-based quadrupoles,[21,32b-d] leading to polar relaxed excited states. Unfortunately, due to the conditional nature of the bistability, excited-state geometry optimizations are not yet capable of reproducing this phenomenon,[32b-d] thus making such calculations mostly irrelevant.

The Lippert-Mataga plots shown in Figure 8 illustrate the overall solvatochromic behavior and offer a way to estimate the variation of the *effective* dipole moment difference between the ground and excited states, provided that a relevant cavity radius is available. From **2V** to **5V**, the gradient steadily increases with the length of the conjugated backbone from 2.2 x 10^3 to 6.2 x 10^3 cm^{-1}. The similarities between compounds **3V** and **5B** in toluene, *vide supra*, are

maintained in more polar solvents, as both compounds exhibit comparable gradients. The substitution of the central thiophene ring of **5V** by an EDOT group in **5VE** leads to an additional rise in the Lippert-Mataga slope, reaching a value of 6.7 x 10^3 cm^{-1}. The evolution of the fluorescence energy with the solvent polarity is also instructive.[21] In fact, the energy shift between cyclohexane and toluene is almost the same for all compounds (*ca.* 600 cm^{-1}), while it increases steadily with the chromophore length in more polar solvents. This reveals two distinct behaviors, and it may be an indication of vanishing or limited localization in non-polar environments and true symmetry breaking in high polarity solvents, again similar to that which has been observed in fluorene-based quadrupoles.[32d]

Two-Photon Absorption (TPA)

Prior to discussing the TPA responses of our chromophores in detail, let us briefly comment on some technical issues to prevent incorrect inferences on TPA structure-property relationships to be drawn. To measure the TPA cross-sections (σ_2), we used the well-known two-photon excited fluorescence (TPEF) method proposed by Xu and Webb,[33] based on measurements relative to a reference compound with known σ_2 values. Thus, the reliability of the derived σ_2 values will be adversely affected by any lack of precision in the reference data, which results from the involved experiments required for the determination of their TPA cross-sections by absolute methods. For one of the most widely used standards, namely fluorescein, comparison of data obtained with different experimental setups, spectrally overlapping, and computed values has already revealed repercussions of imprecise data in the vicinity of 700 nm[32c] and in the 900-1000 nm range.[34] Using fluorescein as a reference with the original data by Xu and Webb,[33] as was done previously for **2V** and **3V**,[14,35] we noticed an intriguing increase of the TPA response of **5VE** on the red edge of the spectrum, while using the more recent value of Makarov, Drobizhev and Rebane[36] led to overall consistent σ_2 values (further details in Supplementary Information. See also Figures S11 and S12). Thus, all TPA cross-sections reported in the manuscript are calculated using the latter data for fluorescein as the reference.

Experimental TPA spectra of series **2V**-**5V** and compounds **5B** and **5VE** are reported in Figure 9 and compared to their respective normalized one-photon absorption spectra. A quadratic dependence of the integrated emission intensity on excitation power was observed, which confirms a two-photon process (Figure S13). For **2V**-**3V**, and to a lesser extent **4V**-**5V** and **5B**, it is clear that the TPA maximum is significantly blue shifted from twice the one-

photon absorption band maximum. This systematic blue shift is confirmed by the calculated TPA spectra for **1V**-**5V** and **5VE** (compare Figures 3 and 10), **2B**-**5B** and **5BE** (compare Figures S8 and S14), and **3T** (compare Figures S9 and S15). This is a direct consequence of the quadrupolar nature of the investigated chromophores, for which inversion symmetry usually leads to a one-photon allowed and TPA forbidden first excited state and a one-photon forbidden and TPA allowed second excited state. X-ray crystallographic data have indeed evidenced inversion symmetry for molecules based on an even number of thiophene rings, whereas the other chromophores show structural features close to it (*vide supra*). Even so, this inversion symmetry and the coexistence of different conformations in solution at ambient temperature will induce a partial breakdown of the selection rules, their reminiscence remains sufficient to be conspicuous, such as that observed for symmetric or slightly asymmetric fluorene based quadrupoles.[1d,32b-d]
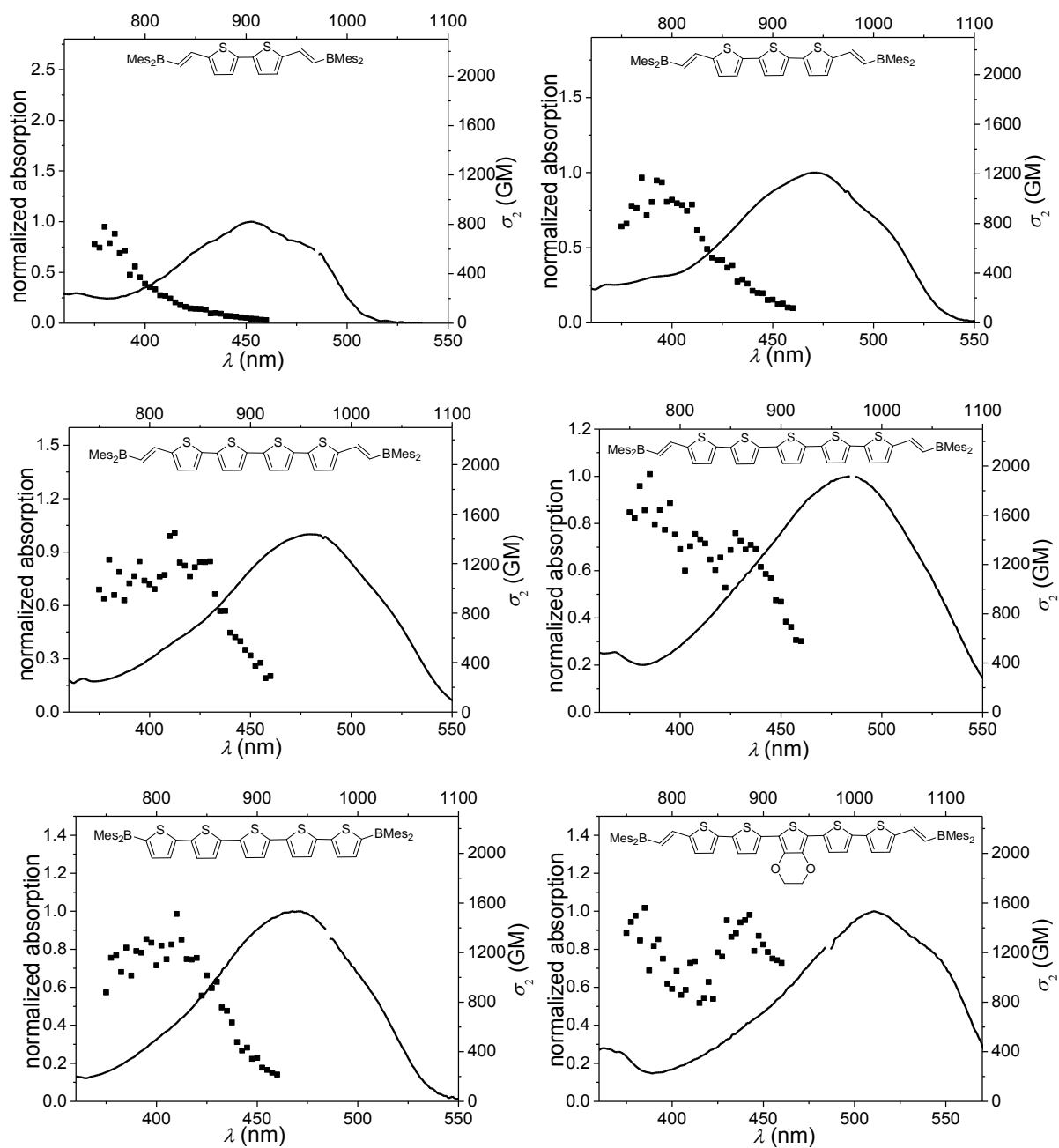
Figure 9. Experimental TPA spectra (squares) and normalized absorption spectra (solid lines) of molecules **2V**-**5V**, **5B** and **5VE** in toluene.
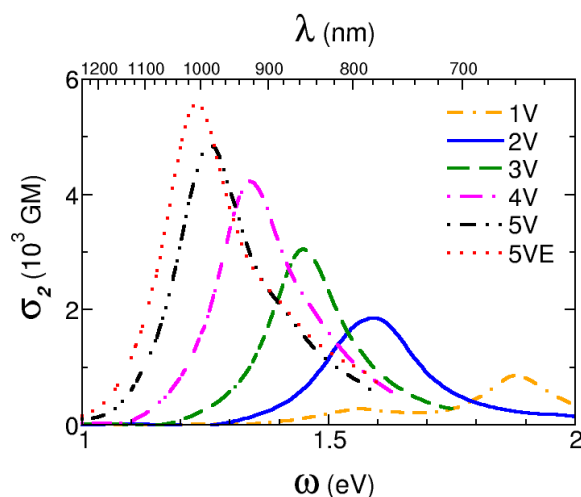
Figure 10. Calculated TPA spectra of molecules **1V**-**5V** and **5VE** in vacuum.

The overall agreement between experiment and theory is good (Figure S16), given that the calculations do not take into account either solvent effects or vibrational contributions and include a fixed bandwidth for all chromophores (Table S7). More importantly, the overestimation of the calculated TPA cross-sections is to be related to the use of B3LYP/6-31G* level of theory for both geometry optimization and properties, which is well known to overestimate conjugation, resulting in reduced BLA values (Table 2). This is illustrated within the well-known 3-state model in which σ_2 is proportional to the fourth power of transition dipole moments.[1d] Indeed, overestimation of transition dipole moments by only 15% leads to TPA cross-sections twice as large. Nevertheless, while absolute transition energies are theoretically underestimated, both for absorption and TPA maxima, the corresponding blue shifts of the TPA maximum relative to double the OPA maximum correlate well between experiment and theory (Figure S16) and give confidence for further discussion of the TPA responses.
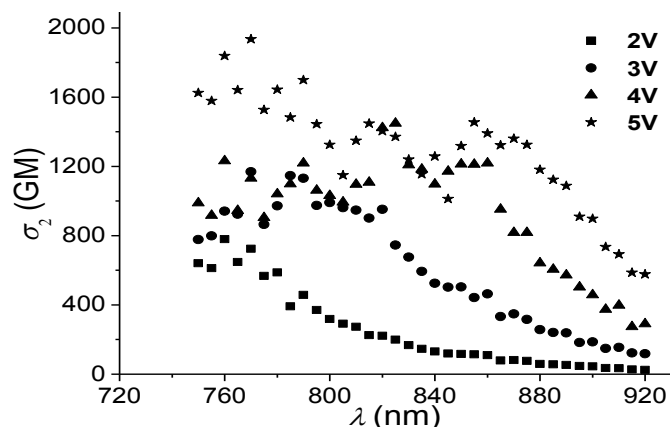

Figure 11. Experimental TPA spectra of **2V**-**5V** in toluene.

The general trends of TPA responses obtained upon elongation of the oligothiophene unit are in accord with those discussed for one-photon absorption: systematic red shift and increase of the TPA amplitude with increasing size (Figures 10 and 11). Calculated spectra for the whole series **2B**-**5B** (Figure S14) show similar trends. A systematic blue shift and reduced amplitudes compared to their vinylene analogues having the same number of thiophene rings is observed (Figure 9). Interestingly, while the one-photon spectra of **5B** were almost identical to that of **3V**, their TPA spectra are noticeably different with a good correspondence between **5B** and **4V** (Figure 12). Indeed, calculations confirm that compounds **nB** and **(n-1)V** have comparable TPA spectra, evidencing an interrelationship between these two series in which the TPA properties of compounds that have an identical number of carbon-carbon double bonds are similar. Thus, the overall behavior is identical for both series and does not manifest any correlation with the different trends observed for the BLA (Table 2).
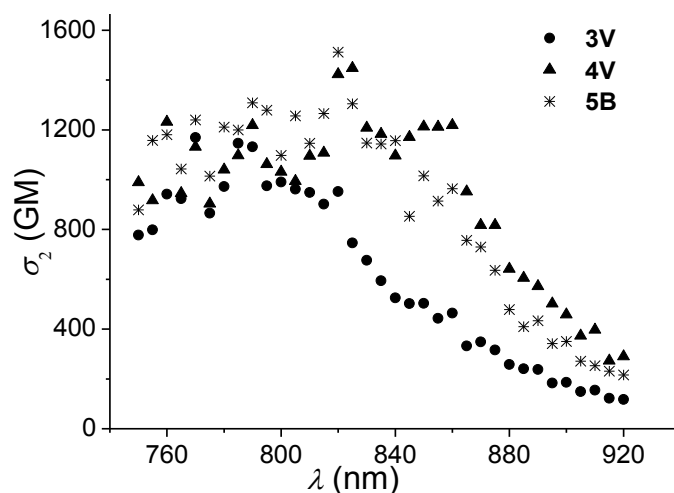

Figure 12. Experimental TPA spectra of **3V**, **4V** and **5B** in toluene.

Experimentally, replacement of the central thiophene ring by an EDOT moiety leads to comparable TPA amplitudes, within experimental uncertainty, and suggests a slight red shift of the first TPA band (Figure 9). Indeed, comparison of calculated TPA spectra of **5V/5VE** (Figure 10), **5B/5BE** (Figure S14) and **3V/3VE** (Figure S15) indicate moderate TPA enhancement of 10% or less, *i.e.* lower than experimental error, with a weak red shift of about 240 cm^{-1}. These trends are consistent with those stated for their one-photon responses (*vide supra*). Interestingly, substitution of the vinylene spacers by ethynylene analogues is predicted to induce a significantly larger (*ca.* 20%) TPA enhancement accompanied by a very small

blue shift (Figure S15). However, unfortunately, in our experience, alkynylBMes$_2$ compounds can be less stable towards hydrolysis than their vinyl analogues.

All chromophores experience similar electronic redistribution upon excitation in the first (low energy) TPA band. This electronic redistribution is illustrated in Figure 13 for **5VE** by the plot of the NTOs associated with the second excited state. Comparison to NTOs relative to the first excited state, relevant for linear absorption (*vide supra*), reveals both the different symmetry and the larger component on the boron atom for the electron whereas the hole remains identical. In terms of molecular orbitals, the electron shows a good correspondence with the LUMO+1. The extensive delocalization of both electron and hole over the molecular backbone translates into TPA enhanced responses upon elongation. For the smallest compounds, up to **2V** and **3B**, the main contributions arise from higher lying excited states with similar electronic redistribution and possible involvement of the mesityl groups.
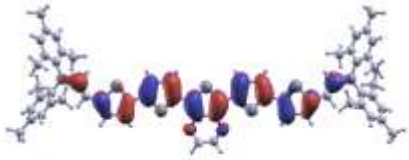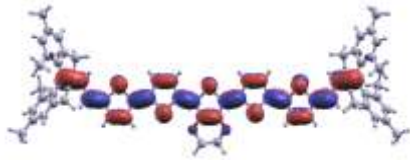
5VE	*Hole*	*Electron*
S$_1$ 2.1 eV 2.8		
S$_2$ 2.5 eV 0.0		

Figure 13. Natural transition orbitals (NTO: Hole/Electron) of chromophores **5VE** associated with the first (S$_1$) and second (S$_2$) excited singlet states, relevant for the first one-photon and two-photon absorption bands, respectively. The left column lists, in sequence, the excited state, associated vertical transition energy and oscillator strength.

Comparison of the TPA activity of our quadrupolar chromophores with related chromophores built from either BMes$_2$[8-13] or oligothiophene moieties[15-20] reveals further information about structure-TPA relationships. We have collated in Table 5, to the best of our knowledge, available data for the best-performing related TPA chromophores, including their TPA cross-sections normalized by molecular weight, σ_2/MW. Corresponding molecular structures are illustrated in Schemes 5 and 6. To ensure appropriate comparison, we have excluded all

reported responses that may be affected by preresonance enhancement, *i.e.* where the excitation wavelength has been tuned close to the lowest energy one-photon resonance. This is particularly important for the oligomers described in Ref. [15], for which it did not seem reasonable to retain EDOT analogues while data for other oligomers were extracted from the low energy part of the reported TPA spectra.

From Table 5 it is clear that, compared to related quadrupoles, our synthetic strategy combining BMes$_2$ with oligothiophenes proves efficient. In fact, all normalized TPA cross-sections (σ_2/MW) are comparable (**2V**) or larger than those previously reported in the literature while the quantum yields remain sizeable. The increase in the length of the oligothiophene spacer appears to be particularly relevant. This prompts comparison to extended oligothiophene-based compounds, such as the all-thiophene dendrimers and the macrocyclic oligothiophenes of Bäuerle and co-workers.[17-19] While leading to sizeable absolute TPA amplitudes with increasing size, the absence of an electron-accepting moiety appears to hinder normalized performances. Further comparison to star-shaped oligothiophenes[20] leads to similar conclusions.

When compared to the branching strategy applied in Ref. [10,12-13] to both quadrupolar[8-10] and dipolar[10,11] analogues, the effectiveness of our BMes$_2$-based compounds is clearly evident. The compounds reported herein have normalized TPA cross-sections approaching that of the best-performing bithiophene push-pull chromophores,[16] despite the large contribution to the molecular weight of the mesityl groups required for stability and applications. Further comparison of σ_2/MW values of our oligothiophene-BMes$_2$ chromophores to other reported BMes$_2$ containing compounds (Table 5),[8-13] shows red-shifted fluorescence maxima, *i.e.* closer to the biological transparency window, especially for the elongated compounds. This makes our oligothiophene-BMes$_2$ good candidates to use in two-photon excited fluorescence microscopy of living cells.
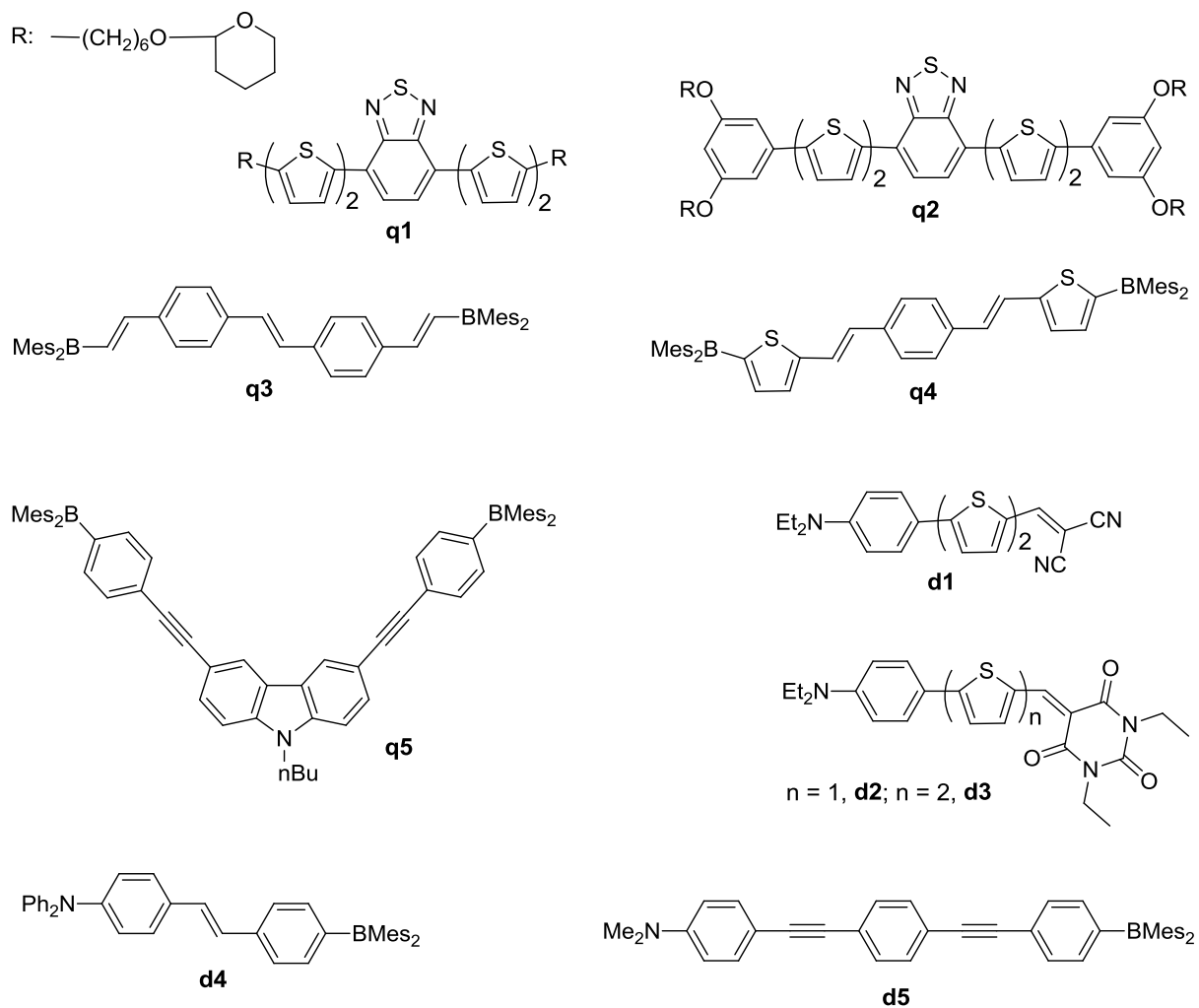
Scheme 5. Structures of the dipolar (**d**) and quadrupolar (**q**) molecules in Table 5.
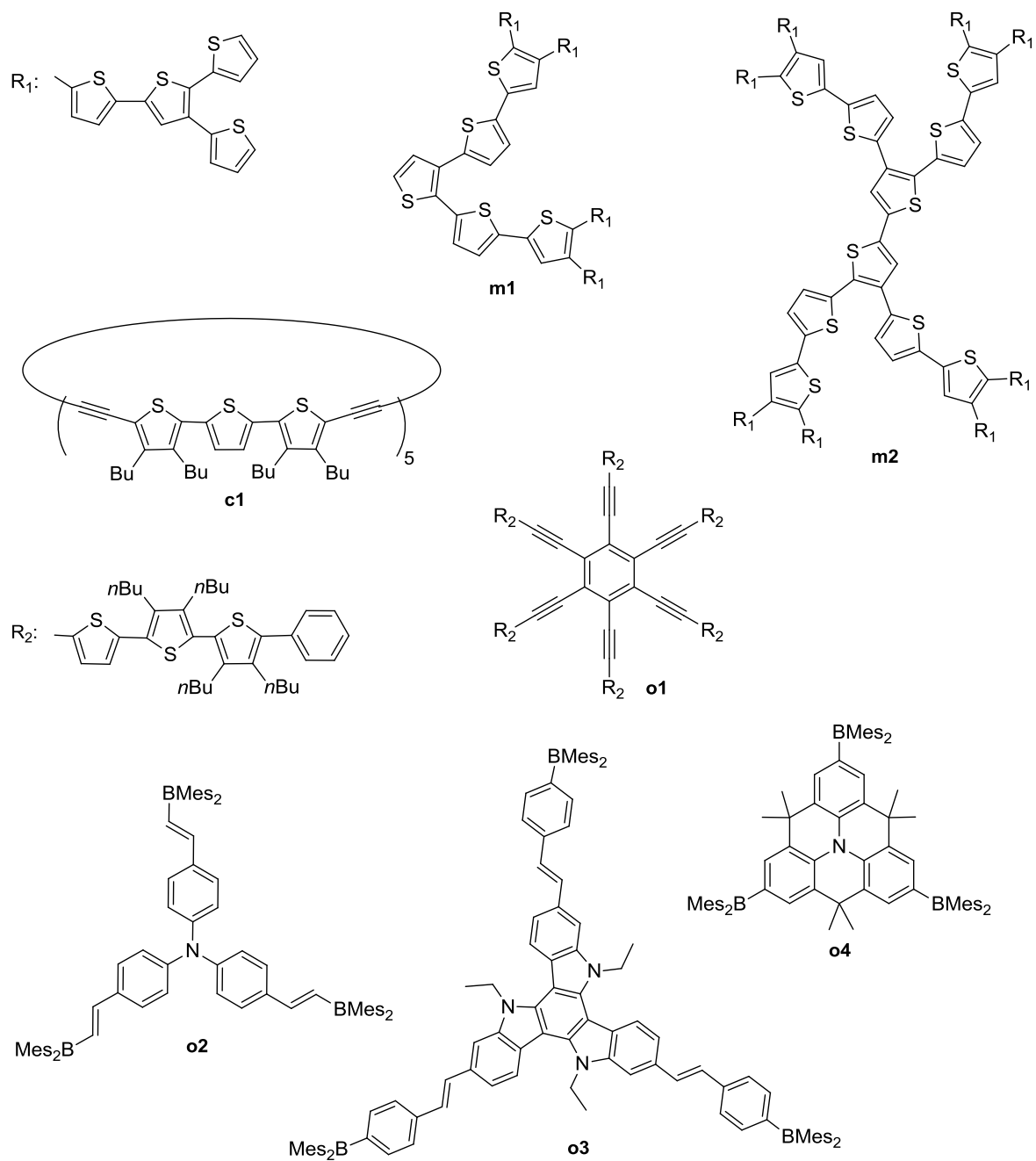
Scheme 6. Structures of the dendrimers (**m**), cyclic (**c**) and octupolar (**o**) molecules in Table 5.

Table 5. Comparison of the reported photophysical data for the best-performing (σ_2/MW) chromophores of different shape and size based on $BMes_2$ and/or oligothiophene moieties. Corresponding molecular structures are given in Scheme 1, 2, 5 and 6.

Class	quadrupoles					
Moieties	oligothiophene and $BMes_2$					
Compound	2V[a]	3V[a]	4V[a]	5V[a]	5B[a]	5VE[a]
λ_{abs}(nm)	453	470	486	487	467	511
ε (10^4 $M^{-1}cm^{-1}$)	5.2	5.7	7.0	7.6	7.9	10
λ_{em} (nm)	509	536	554	563	540	586
Φ_F	0.11	0.20	0.29	0.26	0.26	0.26
σ_2 (GM)	780	1170	1450	1930	1510	1500
@ λ (nm)	760	770	825	770	820	760
σ_2 (GM)/MW	1.1	1.5	1.6	2.0	1.7	1.5

Moieties	oligothiophene		$BMes_2$		
Compound	q1[15][b]	q2[15][b]	q3[8][c]	q4[9][d]	q5[10][a]
λ_{abs} (nm)	517	528	399	435	385
ε (10^4 $M^{-1}cm^{-1}$)	3.0	4.2	7.0	9.3	5.8
λ_{em}(nm)	651	676	447	515	417
Φ_F	0.85	0.44	0.55	NA	0.85
σ_2 (GM)	1200	750	377	850	350
@ λ (nm)	850	850	705	800	770
σ_2 (GM)/MW	1.4	0.5	0.5	1.1	0.45

Class	dipoles				
Moieties	oligothiophene			$BMes_2$	
Compound	d1[16][b]	d2[16][b]	d3[16][b]	d4[11][d]	d5[10][a]
λ_{abs} (nm)	551.5	571.5	587.5	402	367
ε (10^4 $M^{-1}cm^{-1}$)	3.9	6.2	4.6	NA	4.7
λ_{em}(nm)	727	669	781	522	466
Φ_F	0.34	0.09	0.06	0.91	0.89
σ_2 (GM)	780	1240	1600	300	375
@ λ (nm)	790	800	1170	800	780
σ_2 (GM)/MW	2.5	3.0	3.2	0.5	0.7

Class	cyclic	dendrimers		octupoles			
Moieties	oligothiophene			$BMes_2$			
Compound	c1[17][a]	m1[18][d]	m2[19][d]	o1[20][c]	o2[10][a]	o3[12][d]	o4[13][d]
λ_{abs} (nm)	433	382	387	490	440	427	420
ε (10^4 $M^{-1}cm^{-1}$)	NA	NA	NA	19.8	8.5	11	6.4
λ_{em}(nm)	541	542	570	603	480	543	453
Φ_F	0.12	0.05	0.07	0.31	0.73	0.40	0.4
σ_2 (GM)	1470	300	620	2400	1000	2500	260
@ λ (nm)	750	760	800	750	740	820	686
σ_2 (GM)/MW	0.7	0.2	0.2	0.7	0.95	1.7	0.2

[a] in toluene; [b] in CHCl$_3$; [c] in CH$_2$Cl$_2$; [d] in THF.

Conclusions

We have designed and studied experimentally and theoretically quadrupolar chromophores composed of dimesitylboryl π-accepting end-groups, oligothiophene-based donating cores and vinylene spacers. They reveal intense absorption bands (molar extinction coefficient up to 1×10^5 M^{-1} cm^{-1}) in the blue region of the visible spectrum and sizeable quantum yields (0.11-0.29) with a bathochromic shift upon elongation of both absorption and emission. The latter can be tuned from deep green to red. Removal of vinylene spacers allows for further blue shift. Systematic and comparable hyperchromic effects upon elongation with or without vinylene spacers contrast with the trends observed in their BLA. Substitution of a thiophene ring by an EDOT moiety leads to a slight bathochromic shift and hyperchromic effect, evidencing interesting features for potential application in organic solar cells when compared to the DCV5T analogues reported by Bäuerle and co-workers.[30]

Non-linear responses show similar trends with substantial TPA cross-sections of up to 1930 GM in the near-infrared region, the transparent window of biological samples and tissues. This, combined with the red-shifted fluorescence maximum of our oligothiophene-BMes$_2$ chromophores when compared to other reported BMes$_2$-containing compounds, suggests that they may be good candidates to use in two-photon excited fluorescence microscopy of living cells.

Experimental Section:

General manipulations and synthetic techniques

All chemicals were purchased from Sigma-Aldrich, Alfa Aesar, or Acros with the exception of B$_2$pin$_2$, which was kindly provided by AllyChem Co. Ltd. (Dalian, China). All compounds were used without further purification. THF, hexane, Et$_2$O and DMF were dried using an Innovative Technology solvent purification system (SPS). Solvents for chromatography and recrystallization were GPR grade and used without further purification. Dimesitylborane and dimesitylboron fluoride were prepared *via* literature procedures.[37] Precursors **3**,[38] **7**,[39] **8**,[39] **2Sn**,[40] **3Sn**,[41] **3Br**,[42] and 2-(Bpin)thiophene[43] were synthesized according to literature procedures. Other known compounds **2Bpin**,[41, 44] **10a**,[45] **13**,[46] and **14**[47] were synthesized using alternative methods, as described below. NMR experiments were performed on Bruker Avance-400, Varian Mercury-400, Inova-500, VNMRS-600 or VNMRS-700 instruments. ^{1}H and ^{13}C NMR spectra were referenced to residual protiated solvent. MS and HRMS analyses were obtained on Agilent 6890 GC with a 5973 Inert Mass Selective Detector (EI), Bruker

Daltonics Autoflex II TOF/TOF (MALDI), Waters LCT Premier XE equipped with an Acquity UPLC and a lock-mass electrospray ion source, and Waters Xevo QTOF equipped with an Atmospheric Solids Analysis Probe (ASAP). Elemental analyses were carried out on an Exeter Analytical CE-440 analyzer at Durham University. Melting points were measured on a Gallenkamp melting point apparatus and are uncorrected. As is common for organo-BMes$_2$ compounds, several compounds gave carbon analyses that were up to 3% below the calculated value, while hydrogen analyses were satisfactory. This has been ascribed previously to the formation of boron carbide.[10]

(*E*)-[2-(5-bromo-thien-2-yl)vinyl]dimesitylborane (4)

In a glove box, dimesitylborane (400 mg, 1.6 mmol) in THF (50 mL) was added to **3** (180 mg, 0.1 mmol). The solution was stirred for 5 h under nitrogen. After evaporating all of the solvent, the target compound was purified by column chromatography on silica gel with hexane as eluent to give the title compound as a yellow solid (196 mg, 47%). Light yellow crystals were obtained *via* recrystallization from ethanol. m.p. 130-132 °C; ^{1}H NMR (400 MHz, CDCl$_3$): δ = 7.09 (d, J = 17 Hz, 1 H), 7.03 - 6.95 (m, 2 H), 6.84 (m, 5 H), 2.31 (s, 6 H), 2.19 ppm (s, 12 H); ^{13}C{^{1}H} NMR (101 MHz, CDCl$_3$): δ = 146.3, 143.8, 140.8, 138.7, 131.2, 130.0, 128.4, 115.8, 23.4, 21.3 ppm; MS (EI$^+$): m/z: 436 [M^+]; elemental analysis calcd. (%) for C$_{24}$H$_{26}$S: C 65.93, H 5.99; found: C 66.05, H 6.04.

5,5'-bis(Bpin)-2,2'-bithiophene (2Bpin)

Inside a nitrogen-filled glove box, B$_2$pin$_2$ (2.67 g, 10.5 mmol), [Ir(COD)(OMe)]$_2$ (0.100 g, 0.15 mmol), dtbpy (0.08 g, 0.30 mmol) and hexane (30 mL) were added to a Schlenk tube. The tube was taken out of the glove box and 2,2'-bithiophene (1.46 g, 8.8 mmol) was added under a stream of nitrogen. After 30 min of stirring at RT, the stirrer stopped due to sudden precipitation; thus, additional hexane (60 mL) was added. The resulting suspension was stirred at RT for another 15 h before the solvent was removed in vacuum to give a light brown residue. The residue was filtered through a plug of silica using 1:1 CH$_2$Cl$_2$:hexane to give the title compound as a pale green solid (2.91 g, 80%). ^{1}H NMR (400 MHz, CDCl$_3$): δ = 7.52 (d, J = 4 Hz, 2 H), 7.29 (d, J = 4 Hz, 2 H), 1.35 ppm (s, 24 H), ^{13}C{^{1}H} NMR (101 MHz, CDCl$_3$): δ = 143.9, 138.0, 125.6, 84.2, 24.7 ppm; MS (EI$^+$): m/z: 418 [M^+].

(5-bromothiophen-2-yl)dimesitylborane (10a)

Under nitrogen, 2,5-dibromothiophene (1.2 mL, 10 mmol) in dry Et_2O (50 mL) was cooled to -78 °C. nBuLi (1.6 m in hexane, 6.5 mL, 11 mmol) was then added under nitrogen. The mixture was stirred for 0.5 h at -78 °C and then 2 h at room temperature. Then the solution was cooled to -78 °C again, and Mes_2BF (2.7 g, 10 mmol) was added. The solution was stirred for 0.5 h at that temperature and then overnight at room temperature. Water (1 mL) was added to quench the reaction. After removing the solvent, the remaining solid was then purified by column chromatography on silica gel with hexane as eluent to give the title compound as a white solid (2.81 g, 69%). m.p. 136-138 °C; ^{1}H NMR (400 MHz, $CDCl_3$): δ = 7.21 (d, J = 4 Hz, 1 H), 7.17 (d, J = 4 Hz, 1 H), 6.83 (s, 4 H), 2.31 (s, 6 H), 2.13 ppm (s, 12 H); ^{13}C{^{1}H} NMR (101 MHz, $CDCl_3$): δ = 141.0, 140.7, 139.0, 132.6, 128.4, 126.5, 23.6, 21.4 ppm; MS (EI^+): m/z: 413 [M^+]; elemental analysis calcd. (%) for $C_{22}H_{24}BBrS$: C 64.26, H 5.88; found: C 64.23, H 5.92.

(5-iodothiophen-2-yl)dimesitylborane (10b)

To a Schlenk flask charged with 1,4-diiodothiophene (5.0 g, 15 mmol) in 50 mL of dry THF, nBuLi (1.6 m in hexane, 10 mL, 16 mmol) was added dropwise *via* a syringe at -78 °C. The reaction was allowed to warm to room temperature for 1 h and was cooled to -78 °C again and a solution of dimesitylboron fluoride (4.0 g, 15 mmol) in Et_2O (10 mL) was added. The reaction was allowed to warm to room temperature with stirring overnight. The reaction was quenched with HCl_{aq} (1 m, 10 mL), extracted into CH_2Cl_2, dried over Mg_2SO_4, and concentrated *in vacuo*. The residue was purified by column chromatography on silica gel with hexane:CH_2Cl_2 4:1 as eluent to give the title compound as a pale yellow solid (5.8 g, 85%). ^{1}H NMR (400 MHz, $CDCl_3$): δ = 7.28 (d, J = 4 Hz, 1 H), 7.01 (d, J = 4 Hz, 1 H), 6.75 (s, 4 H), 2.23 (s, 6 H), 2.03 ppm (s, 12 H); ^{13}C{^{1}H} NMR (101 MHz, $CDCl_3$): δ = 141.3, 140.9, 139.3, 138.9, 128.3, 89.4, 23.5, 21.2 ppm; MS (ESI^+): m/z: 458 [M^+], 338 [M-Mes$^+$], 211 [M-Mes-I$^+$]; elemental analysis calcd. (%) for $C_{22}H_{24}BIS$: C 57.27, H 5.28; found: C 57.77, H 5.29.

2,5-bis-Bpin-EDOT (12)

Inside a nitrogen-filled glove box, B_2pin_2 (0.51 g, 2 mmol), [Ir(COD)(OMe)]$_2$ (10 mg, 0.015 mmol), hexane (15 mL), and dtbpy (8 mg, 0.030 mmol) were added to a Young's tap tube. The tube was then sealed and taken out of the glove box and 3,4-ethylenedioxy-thiophene (EDOT) (0.142 g, 1 mmol) was added under a stream of nitrogen. The reaction mixture was

stirred at room temperature for 15 h. After filtration and washing with hexane, the title compound was obtained as a white crystalline solid. Yield (0.3 g, 76%). ^{1}H NMR (700 MHz, CDCl$_3$): δ = 4.30 (s, 4 H), 1.35 ppm (s, 24 H); ^{13}C{^{1}H} NMR (176 MHz, CDCl$_3$): δ = 149.2, 110.9, 84.2, 64.9, 25.0 ppm; ^{11}B{^{1}H} NMR (225 MHz, CDCl$_3$): δ = 28.1 ppm; HRMS (ASAP$^+$) calcd. for ^{13}C$_{18}$^{1}H$_{28}$^{11}B$_2$O$_6$^{34}S: 415.1758, found: 415.1749; elemental analysis calcd. (%) for C$_{18}$H$_{28}$B$_2$O$_6$S: C 54.86, H 7.16; found C 54.67, H 7.09.

2,9-diiodo-EDOT (14)

N-Iodosuccinimide (NIS) (3.87 g, 15 mmol) was added to a solution of EDOT (1.07 g, 7.5 mmol) in DMF (50 mL). The mixture was then stirred overnight before being poured into water (150 mL), causing precipitation of a solid. After filtration, a light brown solid was obtained. Recrystallization from CH$_2$Cl$_2$ gave the title compound as light brown crystals (2.09 g, 71%). m.p. 179-184 °C; ^{1}H NMR (400 MHz, CDCl$_3$): δ = 4.26 ppm (s, 4 H); ^{13}C{^{1}H} NMR (101 MHz, CDCl$_3$): δ = 144.0, 65.3, 51.9 ppm; MS (EI$^+$): m/z: 394 [M^+]; elemental analysis calcd. (%) for C$_6$H$_4$I$_2$O$_2$S: C 18.29, H 1.02; found: C 18.43, H 0.91.

5,7-di(thiophen-2-yl)-EDOT (13)

Compounds 2-(Bpin)thiophene (2.1 g, 10 mmol), **14** (1.96 g, 5 mmol), Pd(dppf)Cl$_2$ (0.28 g, 0.34 mmol), and K$_3$PO$_4$·H$_2$O (4.2 g, 20 mmol) were added to a Schlenk flask, followed by dry DMF (60 mL) and distilled water (8 mL) under a stream of nitrogen. The mixture was then heated to 80 °C and stirred overnight. Water (300 mL) was added to quench the reaction, and the mixture was extracted first with Et$_2$O (150 mL x 3), then CHCl$_3$ (400 mL). After evaporating all of the solvent, the remaining oil was then purified by chromatography on silica gel with Et$_2$O-petroleum ether 1:9 as eluent to give the title compound as a yellow solid (0.57 g, 37%). ^{1}H NMR (400 MHz, CDCl$_3$): δ = 7.23-7.22 (m, 4 H), 7.03 (dd, J = 5, 4 Hz, 2 H), 4.39 ppm (s, 4 H); ^{13}C{^{1}H} NMR (101 MHz, CDCl$_3$): δ = 137.6, 134.6, 127.3, 124.1, 123.1, 109.7, 65.1 ppm; MS (EI$^+$): m/z: 306 [M^+]; elemental analysis calcd. (%) for C$_{14}$H$_{10}$O$_2$S$_3$: C 54.88, H 3.29; found: C 54.27, H 3.42.

5,7-bis(5-(trimethylstannyl)thiophen-2-yl)-EDOT (15)

Under nitrogen, compound **13** (0.31 g, 1 mmol) was dissolved in dry THF (10 mL) in a Young's tube. After cooling to -78 °C, nBuLi (1.6 m in hexane, 1.3 mL, 2.1 mmol) was added and the mixture was then stirred for 15 min at that temperature. The solution became cloudy and it was then warmed to room temperature and stirred at RT for 2 h. The reaction mixture

was then cooled to -78 °C and Me$_3$SnCl (0.41 g, 2.05 mmol) was added and the mixture was warmed to room temperature and stirred overnight. Water (100 mL) was added to quench the reaction. It was then extracted into CHCl$_3$ (100 mL x 2), and the organic layer was washed with water (100 mL). After evaporating all of the solvent, the remaining solid was recrystallized from ethanol to give the title compound as a light green crystalline solid (130 mg, 21%). ^{1}H NMR (400 MHz, CDCl$_3$): δ = 7.32 (m, 2 H), 7.10 (d, 84%, ^3J (H,H) = 3 Hz; dd, 16%, $^3J(^{117}$Sn,H) = $^3J(^{119}$Sn,H) = 26 Hz, ^3J(H,H) = 3 Hz, 2 H), 0.38 ppm (s, 84%; d, 16%, $^2J(^{117}$Sn,H) = 55 Hz and d, 16%, $^2J(^{119}$Sn,H) = 58 Hz, 18 H); ^{13}C{^{1}H} NMR (101 MHz, CDCl$_3$): δ = 139.9, 137.2, 136.6, 135.3, 124.0, 109.6, 65.0, -8.2 ppm; MS (ASAP$^+$): m/z: 634 [M^+]; HRMS (ASAP$^+$): calcd. for C$_{20}$H$_{27}$O$_2$S$_3$^{119}Sn$_2$ [M+H]$^+$: 632.9214; found: 632.9199.

5,5'''-bis((*E*)-2-(dimesitylboryl)vinyl)-2,2':5',2'':5'',2'''-quaterthiophene (4V)

Compound **2Sn** (50 mg, 0.105 mmol), Pd(PPh$_3$)$_4$ (4 mg, 0.003 mmol) and compound **4** (94 mg, 0.210 mmol) were dissolved in dry DMF (5 mL). The mixture was heated at 90 °C and stirred for 18 h. Water (50 mL) was added to quench the reaction. Then it was extracted into CHCl$_3$ (50 mL x 3) and the organic layer was washed with water (50 mL x 3), followed by chromatography on silica gel using hexane as eluent to give the title compound as an orange powder (84 mg, 89%). m.p. 250 °C (dec.); ^{1}H NMR (400 MHz, CDCl$_3$): δ = 7.19-7.01 (m, 12 H), 6.84 (s, 8 H), 2.31 (s, 12 H), 2.21 ppm (s, 24 H); ^{13}C{^{1}H} NMR (101 MHz, CDCl$_3$) δ = 144.6, 143.8, 140.9, 139.6, 138.6, 136.7, 136.4, 131.2, 128.4, 125.4, 124.9, 124.8, 23.40, 21.35 ppm; MS (MALDI$^+$): m/z: 878 [M^+]; HRMS (ASAP$^+$) calcd. for C$_{56}$H$_{56}$^{10}B$_2$S$_4$: 876.3524, found: 876.3516; elemental analysis calcd. (%) for C$_{56}$H$_{56}$B$_2$S$_4$: C 76.53, H 6.42, found: C 73.85, H 6.62.

5,5''''-bis((*E*)-2-(dimesitylboryl)vinyl)-2,2': 5',2'': 5'',2''': 5''',2''''-quinquethiophene (5V)

Compound **3Sn** (56 mg, 0.1 mmol), **4** (94.0 mg, 0.210 mmol), and Pd(PPh$_3$)$_4$ (4 mg, 0.003 mmol) were dissolved in dry DMF (5 mL). After degassing, the mixture was heated at 90 °C and stirred overnight under nitrogen. The solution was added to water (20 mL), and then extracted into CHCl$_3$ (20 mL x 3) and dried over MgSO$_4$. After filtration and evaporating all of the solvent, **5V** was purified by chromatography on silica gel starting with petroleum ether, and increasing the polarity to CHCl$_3$:petroleum ether 1:4 as eluent, to give the title compound as an orange powder (86 mg, 89%). ^{1}H NMR (400 MHz, CDCl$_3$): δ = 7.20-7.02 (m, 14 H), 6.84 (s, 8H), 2.31 (s, 12 H), 2.21 ppm (s, 24 H); ^{13}C{^{1}H} NMR (101 MHz, CDCl$_3$): δ = 144.6, 143.7, 142.2, 140.8, 139.7, 138.6, 136.8, 136.3, 136.2, 131.2, 128.4,

125.4, 124.9, 124.8, 23.5, 21.4 ppm; MS (MALDI$^+$): m/z: 960; HRMS (ASAP$^+$): calcd. for C$_{60}$H$_{58}$^{10}B$_2$S$_5$: 958.3401, found: 958.3403; elemental analysis calcd. (%) for C$_{60}$H$_{58}$B$_2$S$_5$: C 74.98, H 6.08; found: C 73.49, H 6.21.

5,7-bis(5'-((E)-2-(dimesitylboryl)vinyl)-[2,2'-bithiophen]-5-yl)-EDOT (5VE)

Compound **15** (63 mg, 0.1 mmol), **4** (50 mg, 0.23 mmol), and Pd(PPh$_3$)$_4$ (3 mg, 0.003 mmol) were dissolved in DMF (5 mL) in a Young's tube in a nitrogen-filled glove box. The tube was sealed, taken out the glove box, and heated at 90 °C with stirring overnight. The reaction solution was poured into water (40 mL), which caused precipitation of a solid. After filtration, the solid was purified by chromatography on silica gel using CH$_2$Cl$_2$:petroleum ether 1:3 as eluent to give the title compound as a red powder (62 mg, 66%). ^{1}H NMR (400 MHz, CDCl$_3$): δ = 7.19-7.01 (m, 12 H), 6.84 (s, 8 H), 2.31 (s, 12 H), 2.21 ppm (s, 24 H); ^{13}C{^{1}H} NMR (101 MHz, CDCl$_3$): δ = 144.8, 143.3, 142.3, 140.8, 140.2, 138.6, 138.2, 137.5, 135.7, 134.4, 131.3, 128.4, 124.9, 124.3, 123.9, 110.1, 65.2, 23.4, 21.3 ppm; MS (MALDI$^+$): m/z: 1018; HRMS (ASAP$^+$) calcd. for C$_{62}$H$_{60}$^{10}B$_2$O$_2$S$_5$: 1016.3456, found: 1016.3427; elemental analysis calcd. (%) for C$_{62}$H$_{60}$B$_2$O$_2$S$_5$: C 73.07, H 5.93; found: C 70.89, H 6.17.

5,5''''-bis(dimesitylboryl)-2,2': 5',2'': 5'',2''': 5''',2''''-quinquethiophene (5B)

Compound **3Sn** (86 mg, 0.15 mmol), **10a** (150 mg, 0.34 mmol), and Pd(PPh$_3$)$_4$ (4 mg, 0.004 mmol) were dissolved in DMF (5 mL) in a Young's tube in a nitrogen-filled glove box. Then the Young's tube was sealed, heated at 90 °C and stirred overnight. Water (100 mL) was added to quench the reaction, causing precipitation of a solid. After filtration, the residue was purified by chromatography on silica gel first using petroleum ether and then CHCl$_3$:petroleum ether 1:5 as eluent to give the title compound as a red solid (118 mg, 87%). ^{1}H NMR (400 MHz, CDCl$_3$): δ = 7.36 (d, J = 4 Hz, 2H), 7.29 (d, J = 4 Hz, 2H), 7.18 (d, J = 4 Hz, 2H), 7.08 (m, 4H), 6.84 (s, 8H), 2.32 (s, 12H), 2.15 ppm (s, 24H); ^{13}C{^{1}H} NMR (126 MHz, CDCl$_3$): δ = 149.51, 149.45, 141.8, 141.3, 141.1, 138.8, 137.3, 136.5, 136.4, 128.4, 126.0, 124.9, 124.9, 23.7, 21.5 ppm; MS (MALDI$^+$): m/z: 908 [M^+]; HRMS (ASAP$^+$) calcd. for C$_{56}$H$_{54}$^{10}B$_2$S$_5$: 906.3088, found: 906.3064; elemental analysis calcd. (%) for C$_{56}$H$_{54}$B$_2$S$_5$: C 74.00, H 5.99; found: C 71.03, H 5.81.

Alternative method for the synthesis of 5B

Dibromoterthiophene **3Br** (40 mg, 0.1 mmol), **8** (92 mg, 0.2 mmol) and K$_3$PO$_4$·H$_2$O (85 mg, 0.4 mmol) were added to a Young's tube. The tube was taken in to the glove box where

Pd(dppf)Cl$_2$ (33 mg, 0.004 mmol) and DMF (2 mL) were added. The tube was sealed and taken out of the glove box where H$_2$O (0.2 mL) was added under a stream of N$_2$. The tube was sealed and stirred at room temperature for 26 h and then heated to 60 °C for 2 h. Water (40 mL) was added to the reaction, the mixture was then extracted with diethyl ether (5 x 20 mL) and ethyl acetate (3 x 20 mL). The combined organic layers were dried over MgSO$_4$, filtered, and concentrated yielding a dark red oily solid which was purified by flash chromatography on silica gel with CH$_2$Cl$_2$:hexane 1:19 as the eluent to give the title compound as a red solid (80 mg, 88%).

X-ray crystallography

Crystals of **2V** were obtained from hexane, and those of **4V** and **5B** were grown by slow diffusion of methanol into toluene solutions. Crystals were coated in perfluoropolyether oil, and mounted on glass fibers. Data were collected at 120 K on Bruker 3-circle diffractometers with either SMART 1000 (**7**, **8**, **10b**) or SMART 6000 CCD area detectors, using Mo-Kα radiation (λ = 0. 71073 Å). The crystal structures were solved by direct methods and refined by full-matrix least squares (non-hydrogen atoms in anisotropic approximation, hydrogen atoms in 'riding' model) using OLEX2 and SHELXTL software.[48] CCDC 985867-985874 contain the supplementary crystallographic data for this paper. These data can be obtained free of charge from The Cambridge Crystallographic Data Centre via www.ccdc.cam.ac.uk/data_request/cif.

Photophysical measurements

One-photon absorption and emission spectroscopy, fluorescence quantum yields and lifetimes

The UV-visible absorption spectra were measured in standard 1 x 1 cm quartz cuvettes using an Agilent 8453 diode-array UV-visible spectrophotometer. Fluorescence spectra and quantum yields were measured using a Horiba Jobin-Yvon Fluoromax-3 spectrophotometer, with a concentration of *ca.* 10^{-6} m to minimize reabsorption. The fluorescence quantum yield of **3V** was measured using an integrating sphere on a Horiba Jobin-Yvon Fluorolog-3-22-tau spectrophotometer by a previously reported method,[49] to be 0.18, which matches within experimental error (*ca.* ±10%) the value reported previously (Φ_F = 0.20).[14] The fluorescence quantum yields of all other compounds were measured against the reported value of **3V** in toluene (Φ_F = 0.20) for easier comparison with earlier data. The emission band of **3V** overlaps

most of the emission spectra of the compounds measured in this work, which minimizes the error of the measurements.

The fluorescence lifetimes were measured in optically dilute ($A < 0.15$) toluene solution by time-correlated single-photon counting (TCSPC) using 450 nm excitation. The excitation source used was the 2nd harmonic of a mode-locked (900 nm), cavity dumped (APE Pulse switch) Ti:sapphire laser (Coherent MIRA), pumped by the 2nd harmonic (532 nm) of a continuous wave Nd:YAG laser (Coherent Verdi V6) at a power of 4.5 W. The pulse characteristics were: a temporal full width at half maximum (FWHM) of ~150 fs at a repetition rate of 4 MHz. The fluorescence emission was collected at right angles to the excitation source, with the emission wavelength selected using a monochromator (Jobin-Yvon TRIAX 190) and detected under magic-angle conditions by a cooled photomultiplier-tube module (IBH TBX-04). The power of the laser was modulated to give a detector count rate <20 kHz. The instrument response function (IRF) was ~200 ps FWHM, measured using toluene as the scattering sample. Iterative reconvolution of the IRF with a decay function and non-linear least-squares analysis were used to analyze the data. The quality of the fit was judged by visual inspection of the residuals and autocorrelated residuals, and by the calculated values of χ^2 and the Durbin-Watson parameter. Fitting with a single decay function gave acceptable results in all cases. Estimated error ±5%.

Two-photon absorption (TPA) spectroscopy

Two-photon cross-sections were measured using the femtosecond two-photon-excited fluorescence method.[33] The tunable fundamental output of the same Ti:sapphire laser described above for TCSPC measurements was used as an excitation source. The pulse characteristics were: a temporal full width at half maximum (FWHM) of ~150 fs; average power 5-35 mW at a repetition rate of ~2.5 MHz, giving average energies of 2-14 nJ per pulse. A variable ND filter (Edmund Optics) mounted on a translation stage was used to control the light intensity incident on the sample, with the power monitored by splitting the beam to a photodiode of known response, calibrated against a free standing power meter. Gold mirrors, highly reflective of near-IR radiation, were used with a 20x objective (Olympus LWD C A20) to focus the source onto the sample. Samples were prepared with $A = 0.2$-0.3 at their absorption maximum (concentrations: *ca.* 10^{-6} m) in quartz cuvettes of path length, $l = 1$ cm. The two-photon excited fluorescence emission was collected with a dichroic mirror (Semrock FF735) and detected with a 100 μm core fiber-optic cable coupled CCD

spectrograph (Avantes Avaspec 2048FT) fitted with a 670 nm narrow band pass filter to remove extraneous laser light. TPA cross-sections (σ_2) were measured relative to a reference, as per the standard methodology of Rebane and co-workers[36] (*vide supra* and Supplementary Information), using the equation:

$$\sigma_2^S = \frac{\sigma_2^R \Phi_F^R c^R n^S F^S(\lambda)}{\Phi_F^S c^S n^R F^R(\lambda)}$$

The superscripts R and S refer to the reference and sample respectively, Φ_F is the one-photon photoluminescence quantum yield, c is the concentration, n is the solvent refractive index and $F(\lambda)$ is the integrated two-photon emission spectrum. The sample and reference were recorded under identical pulse conditions. The concentration of the reference fluorescein was measured by UV-visible spectroscopy using $\varepsilon_{492\text{ nm}} = 88\,000$ dm^3 mol^{-1} cm^{-1} and interpolated literature values[36,50] of σ_2 for fluorescein in 0.1 m NaOH with $\Phi_F = 0.9$ were used. The wavelength of the laser was tuned step-wise to allow the full TPA spectrum to be obtained in 5 nm steps in the range 750 to 920 nm. The system was calibrated to correct for the dark noise of the detector and the photoluminescence spectrum was typically averaged over 100 measurements of 100 ms integration time. In-house software written in LabVIEW 8.6 (National Instruments) was used for data collection and analysis. Estimated error ±20%.

Computational details

We used quantum chemical approaches, as implemented in the Gaussian 03 or 09 packages,[51] to model all chromophores. Calculations were performed in vacuum and were limited to properties related to the ground state geometry: geometry optimization and related ground state (GS) properties, one and two-photon absorption related to the electronically excited states (ES). Optical spectra were obtained employing the density matrix formalism for non-linear optical responses as proposed by Tretiak and Chernyak.[52] We did not model relaxed excited states to simulate fluorescence as they are expected to undergo localization prior to emission (vide supra) that cannot be reproduced yet by state-of-the-art quantum chemical approaches.[32b-d] This rules out any modern approaches, such as that proposed by Jacquemin and co-workers,[53] aiming at computing accurate transition energies in solution for quantitative comparison with experimental data. Furthermore, accounting for solvent effects when calculating TPA spectra is not straightforward as the local field correction is not properly described by a simple local field factor to the fourth power.[1d] Given the approximations introduced by the use of inexact DFT functionals, one may reach better

quantitative results with low cost calculations in vacuum, as has been shown for the hybrid B3LYP functional.[1d]

Different levels of theory and starting conformations have been tested for geometry optimization in vacuum using the 6-31G* basis set. As our main purpose was to investigate NLO properties, we used the bond length alternation as a quality factor. As expected, Hartree-Fock calculations significantly overestimate the BLA, whereas DFT calculations with the BP86 functional, used in previous work on B(Mes)$_2$-based chromophores,[14] significantly underestimate this parameter (Table S4). DFT with the hybrid functional B3LYP was found to lead to a good compromise; even so, the smaller BLA, as compared to that derived from X-ray diffraction structures, highlights its tendency to overestimate conjugation (Table 2 and S4). This could be partly cured using long-range corrected hybrids, such as the CAM-B3LYP functional (Table S5), but we preferred keeping the same level of theory both for geometry optimization and optical properties and to concentrate on overall trends.

The crystal structures reveal both *cisoid* and *transoid* conformers, with a preference for *transoid* when inversion symmetry matches molecular structure (*i.e.* even number of thiophene rings for all *trans* conformation). We have verified, in the case of **2V**, that both conformers are energetically close enough to coexist in solution at room temperature. In addition, the all *trans* conformers, where adjacent rings of the oligothiophene backbones have opposite orientations, have been compared to their all *cis* analogues. While for the shortest compound, namely **2V**, the energy difference is within the energy of thermal activation at RT ($k_B T_{\mathrm{RT}}$), it increases with the number of thiophene rings up to about 10 $k_B T_{\mathrm{RT}}$ for **5V** and **5VE** in favor of the all *trans* conformation. Thus, for consistency, we retained conformations with all *trans*-thiophene backbones and *cisoid*-vinylBMes$_2$/thiophene end groups for all chromophores of interest. Calculations were performed in vacuum at the (TD-)B3LYP/6-31G*//B3LYP/6-31G* level of theory, in conventional quantum chemical notation "single point//optimization level". Natural transition orbitals[28] (NTO) analysis has been used to characterize electronic transitions. NTOs offer a compact representation of excited states, particularly useful when there is no dominant amplitude of a pair of occupied and empty individual molecular orbitals (*e.g.* HOMO and LUMO) to the total electronic transition. NTO pairs consist of an excited particle (or electron-orbital) and empty hole (or hole-orbital) illustrating the electronic redistribution upon (de-)excitation. Excited-state electronic-structure analyses, both optical response and NTOs, were performed for 20 singlet excited states (ES).

Comparison of 20 and 60 ES at the TD-B3LYP/6-31G//B3LYP/6-31G* level of theory showed that 20 ES are sufficient, especially for the calculations of TPA spectra (Figure S17). All theoretical TPA spectra have been computed following the computational scheme introduced in Ref. [1d]. The damping factor, introduced to simulate the finite linewidth in the resonant spectra, has been fixed to 0.17 eV, derived from the experimental bandwidths (Table S7). Figures visualizing molecular geometries and NTOs were obtained with XCrySDen.[54]

Acknowledgements

References

[1] a) B. Strehmel, V. Strehmel, *Adv. Photochem.* **2007**, *29*, 111-354; b) M. Rumi, S. Barlow, J. Wang, J. W. Perry, S. R. Marder, *Adv. Polym. Sci.* **2008**, *213*, 1-95; c) G. S. He, L. S. Tan, Q. Zheng, P. N. Prasad, *Chem. Rev.* **2008**, *108*, 1245-1330; d) F. Terenziani, C. Katan, E. Badaeva, K. Tretiak, M. Blanchard-Desce, *Adv. Mater.* **2008**, *20*, 4641-4678; e) H. M. Kim, B. R. Cho, *Chem. Commun.* **2009**, 153-164; f) M. Pawlicki, H. A. Collins, R. G. Denning, H. L. Anderson, *Angew. Chem. Int. Ed.* **2009**, *48*, 3244-3266.

[2] a) W. Denk, J. H. Strickler, W. W. Webb, *Science* **1990**, *248*, 73-76; b) A. Specht, F. Bolze, Z. Omran, J. F. Nicoud, M. Goeldner, *HFSP J.* **2009**, *3*, 255-264; c) H. M. Kim, B. R. Cho, *Chem. Asian J.* **2011**, *6*, 58-69; d) G. Bort, T. Gallavardin, D. Ogden, P. I. Dalko, *Angew. Chem. Int. Ed.* **2013**, *52*, 4526-4537; e) Z. P. Feng, W. T. Zhang, J. M. Xu, C. Gauron, B. Ducos, S. Vriz, M. Volovitch, L. Jullien, S. Weiss, D. Bensimon, *Rep. Prog. Phys.* **2013**, *76*, 072601.

[3] a) B. C. Das, P. Thapa, R. Karki, C. Schinke, S. Das, S. Kambhampati, S. K. Banerjee, P. van Veldhuizen, A. Verma, L. M. Weiss, T. Evans, *Future Med. Chem.* **2013**, *5*, 653-676; b) A. R. Martin, J. J. Vasseur, M. Smietana, *Chem. Soc. Rev.* **2013**, *42*, 5684-5713.

[4] K. Miwa, Y. Furusho, E. Yashima, *Nat. Chem.* **2010**, *2*, 444-449.

[5] a) C. D. Entwistle, T. B. Marder, *Angew. Chem.* **2002**, *114*, 3051-3056; *Angew. Chem. Int. Ed.* **2002**, *41*, 2927-2931; b) C. D. Entwistle, T. B. Marder, *Chem. Mater.* **2004**, *16*, 4574-4585; c) S. Yamaguchi, A. Wakamiya, *Pure Appl. Chem.* **2006**, *78*, 1413-1424; d) F. Jäkle, *Coord. Chem. Rev.* **2006**, *250*, 1107-1121; e) Z. Yuan, J. C. Collings, N. J. Taylor, T. B. Marder, C. Jardin, J.-F. Halet, *J. Solid State Chem.* **2000**, *154*, 5-12; f) Z. M. Hudson, S. Wang, *Acc. Chem. Res.* **2009**, *42*, 1584-1596; g) S. Yamaguchi, T. Shirasaka, K. Tamao, *Org. Lett.* **2000**, *2*, 4129-4132; h) C.-H. Zhao, A. Wakamiya, Y. Inukai, S. Yamaguchi, *J. Am. Chem. Soc.* **2006**, *128*, 15934-15935; i) L. Weber, V. Werner, M. A. Fox, T. B. Marder, S. Schwedler, A. Brockhinke, H.-G. Stammler, B. Neumann, *Dalton Trans.* **2009**, 1339-1351; j) L. Weber, V. Werner, M. A. Fox, T. B. Marder, S. Schwedler, A. Brockhinke, H.-G. Stammler, B. Neumann, *Dalton Trans.* **2009**, 2823-2831; k) L. Weber, D. Eickhoff, T. B. Marder, M. A. Fox, P. J. Low, A. D. Dwyer, D. J. Tozer, S. Schwedler, A. Brockhinke, H.-G. Stammler, B. Neumann, *Chem. Eur. J.* **2012**, *18*, 1369-1382.

[6] P. J. Grisdale, J. L. R. Williams, M. E. Glogowski, B. E. Babb, *J. Org. Chem.* **1971**, *36*, 544-549.

[7] a) Z. Liu, Q. Fang, D. Wang, G. Xue, W. Yu, Z. Shao, M. Jiang, *Chem. Commun.* **2002**, 2900-2901; b) D. Cao, Z. Liu, Q. Fang, G. Xu, G. Liu, W. Yu, *J. Organomet. Chem.* **2004**, *689*, 2201-2206; c) D. Cao, Z. Liu, G. Zhang, G. Li, *Dyes Pigments* **2009**, *81*, 193-196; d) D. Cao, Z. Liu, G. Li, G. Liu, G. Zhang, *J. Mol. Struct.* **2008**, *874*, 46-50.

[8] M. Charlot, L. Porrès, C. D. Entwistle, A. Beeby, T. B. Marder, M. Blanchard-Desce, *Phys. Chem. Chem. Phys.* **2005**, *7*, 600-606.

[9] a) Z. Liu, Q. Fang, D. Cao, D. Wang, G. Xu, *Org. Lett.* **2004**, *6*, 2933-2936; b) Z.-Q. Liu, M. Shi, F-Y. Li, Q. Fang, Z.-H. Chen, T. Yi, C.-H. Huang, *Org. Lett.* **2005**, *7*, 5481-5484.

[10] J. C. Collings, S. Y. Poon, C. L. Droumaguet, M. Charlot, C. Katan, L. O. Pålsson, A. Beeby, J. A. Mosely, H. M. Kaiser, D. Kaufmann, W. Y. Wong, M. Blanchard-Desce, T. B. Marder, *Chem. Eur. J.* **2009**, *15*, 198-208.

[11] Z. Liu, Q. Fang, D. Wang, D. Cao, G. Xue, W. Yu, H. Lei, *Chem. Eur. J.* **2003**, *9*, 5074-5084.

[12] L. Ji, Q. Fang, M.-S. Yuan, Z.-Q. Liu, Y.-X. Shen, H.-F. Chen, *Org. Lett.* **2010**, *12*, 5192-5195.

[13] N. S. Makarov, S. Mukhopadhyay, K. Yesudas, J.-L. Brédas, J. W. Perry, A. Pron, M. Kivala, K. Müllen, *J. Phys. Chem. A* **2012**, *116*, 3781-3793.

[14] C. D. Entwistle, J. C. Collings, A. Steffen, L.-O. Pålsson, A. Beeby, D. Albesa-Jové, J. M. Burke, A. S. Batsanov, J. A. K. Howard, J. A. Mosely, S.-Y. Poon, W.-Y. Wong, F. Ibersiene, S. Fathallah, A. Boucekkine, J.-F. Halet, T. B. Marder, *J. Mater. Chem.* **2009**, *19*, 7532-7544.

[15] S. Ellinger, K. R. Graham, P. Shi, R. T. Farley, T. T. Steckler, R. N. Brookins, P. Taranekar, J. Mei, L. A. Padilha, T. R. Ensley, H. Hu, S. Webster, D. J. Hagan, E. W. van Stryland, K. S. Schanze, J. R. Reynolds, *Chem. Mater.* **2011**, *23*, 3805-3817.

[16] E. Genin, V. Hugues, G. Clermont, C. Herbivo, M. C. R. Castro, A. Comel, M. M. M. Raposob, M. Blanchard-Desce, *Photochem. Photobiol. Sci.* **2012**, *11*, 1756-1766.

[17] A. Bhaskar, G. Ramakrishna, K. Hagedorn, O. Varnavski, E. Mena-Osteritz,

P. Bäuerle, T. Goodson III, *J. Phys. Chem. B* **2007**, *111*, 946-954.

[18] G. Ramakrishna, A. Bhaskar, P. Bäuerle, T. Goodson III, *J. Phys. Chem. A* **2008**, *112*, 2018-2026.

[19] M. R. Harpham, O. Süzer, C.-Q. Ma, P. Bäuerle, T. Goodson III, *J. Am. Chem. Soc.* **2009**, *131*, 973-979.

[20] T. Narita, M. Takase, T. Nishinaga, M. Iyoda, K. Kamada, K. Ohta, *Chem. Eur. J.* **2010**, *16*, 12108-12113.

[21] F. Terenziani, A. Painelli, C. Katan, M. Charlot, M. Blanchard-Desce, *J. Am. Chem. Soc.* **2006**, *128*, 15742-15755.

[22] I. A. I. Mkhalid, J. H. Barnard, T. B. Marder, J. M. Murphy, J. F. Hartwig, *Chem. Rev.* **2010**, *110*, 890-931.

[23] N. Wang, Z. M. Hudson, S. Wang, *Organometallics* **2010**, *29*, 4007-4011.

[24] F. H. Allen, O. Kennard, D. G. Watson, L. Brammer, A. G. Orpen, R. J. Taylor, *J. Chem. Soc. Perkin Trans. 2* **1987**, S1-S19.

[25] a) Z. Yuan, N. J. Taylor, T. B. Marder, I. D. Williams, S. K. Kurtz, L. T. J. Cheng, *J. Chem. Soc. Chem. Commun.* **1990**, 1489-1492; b) Z. Yuan, N. J. Taylor, R. Ramachandran, T. B. Marder, *Appl. Organometal. Chem.* **1996**, *10*, 305-316 ; c) C. D. Entwistle, T. B. Marder, P. S. Smith, J. A. K. Howard, M. A. Fox, S. A. Mason, *J. Organomet. Chem.* **2003**, *680*, 165–172; d) C. D. Entwistle, A. S. Batsanov, J. A. K. Howard, M. A. Fox, T. B. Marder, *Chem. Commun.* **2004**, 702-703; e) Z. Yuan, C. D. Entwistle, J. C. Collings, D. Albesa-Jové, A. S.

Batsanov, J. A. K. Howard, H. M. Kaiser, D. E. Kaufmann, S.-Y. Poon, W.-Y. Wong, C. Jardin, S. Fatallah, A. Boucekkine, J.-F. Halet, T. B. Marder, *Chem. Eur. J.* **2006**, *12*, 2758-2771; f) A. G. Crawford, Z. Q. Liu, I. A. I. Mkhalid, M. H. Thibault, N. Schwarz, G. Alcaraz, A. Steffen, J. C. Collings, A. S. Batsanov, J. A. K. Howard, T. B. Marder, *Chem. Eur. J.* **2012**, *18*, 5022-5035.

[26] C. B. Gorman, S. R. Marder, *Proc. Natl. Acad. Sci.* **1993**, *90*, 11297-11301.

[27] A. Sundararaman, K. Venkatasubbaiah, M. Victor, L. N. Zakharov, A. L. Rheingold, F. Jäkle, *J. Am. Chem. Soc.* **2006**, *128*, 16554-16565.

[28] R. L. Martin, *J. Chem. Phys.* **2003**, *118*, 4775-4777.

[29] a) T. Noda, Y. Shirota, *J. Am. Chem. Soc.* **1998**, *120*, 9714-9715; b) T. Noda, H. Ogawa, Y. Shirota, *Adv. Mater.* **1999**, *11*, 283-285; c) Y. Shirota, *J. Mater. Chem.* **2000**, *10*, 1-25; d) T. Noda, Y. Shirota, *J. Lumin.* **2000**, *87*, 1168-1170; e) A. J. Mäkinen, I. G. Hill, T. Noda, Y. Shirota, Z. H. Kafafi, *Appl. Phys. Lett.* **2001**, *78*, 670-672; f) A. J. Mäkinen, I. G. Hill, M. Kinoshita, T. Noda, Y. Shirota, Z. H. Kafafi, *J. Appl. Phys.* **2002**, *91*, 5456-5461.

[30] R. Fitzner, E. Mena-Osteritz, A. Mishra, G. Schulz, E. Reinold, M. Weil, C. Körner, H. Ziehlke, C. Elschner, K. Leo, M. Riede, M. Pfeiffer, C. Uhrich, P. Bäuerle, *J. Am. Chem. Soc.* **2012**, *134*, 11064-11067.

[31] F. Terenziani, C. Sissa, A. Painelli, *J. Phys. Chem. B* **2008**, *112*, 5079-5087.

[32] a) R. Stahl, C. Lambert, C. Kaiser, R. Wortmann, R. Jakober, *Chem. Eur. J.* **2006**, *12*, 2358-2370; b) C. Katan, F. Terenziani, O. Mongin, M. H. V. Werts, L. Porrès, T. Pons, J. Mertz, S. Tretiak, M. Blanchard-Desce, *J. Phys. Chem. A* **2005**, *109*, 3024-3037; c) C. Katan, S. Tretiak, M. H. V.Werts A. J. Bain, R. J. Marsh, N. Leonczek, N. Nicolaou, E. Badaeva, O. Mongin, M. Blanchard-Desce, *J. Phys. Chem. B* **2007**, *111*, 9468-9483; d) C. Katan, M. Charlot, O. Mongin, C. L. Droumaguet, V. Jouikov, F. Terenziani, E. Badaeva, S. Tretiak, M. Blanchard-Desce, *J. Phys. Chem. B* **2010**, *114*, 3152-3169 and references therein.

[33] C. Xu, W. W. Webb, *J. Opt. Soc. Am. B* **1996**, *13*, 481-491.

[34] C. Sissa, V. Parthasarathy, D. Drouin-Kucma, M. H. V. Werts, M. Blanchard-Desce, F. Terenziani, *Phys. Chem. Chem. Phys.* **2010**, *12*, 11715-11727.

[35] The change of reference data does not fully explain the significant difference in TPA amplitudes between the data already published for **3V** [14] and the present values that are found to be lower by a factor of about two. Experimental setup and conditions remaining the same for the two measurements, we have as yet no explanation for this discrepancy. Nevertheless, the overall trends are consistent with calculated spectra, namely systematic

behavior upon elongation, and we are confident of trends and that we are free of any overestimation of the present data.

[36] N. S. Makarov, M. Drobizhev, A. Rebane, *Opt*. *Express* **2008**, *16*, 4029-4047.

[37] A. Pelter, K. Smith, H. C. Brown, *Borane Reagents*, Academic Press, London, **1988**, pp. 428-429.

[38] E. G. A. Notaras, N. T. Lucas, M. G. Humphrey, *Organometallics* **2003**, *22*, 3659-3670.

[39] Y. Chen, D. Cao, S. Wang, C. Zhang, Z. Liu, *J. Mol. Struct.* **2010**, *969*, 182-186.

[40] H. H. Fong, V. A. Pozdin, A. Amassian, G. G. Malliaras, D.-M. Smilgies, M. He, S. Gasper, F. Zhang, M. Sorensen, *J. Am. Chem. Soc.* **2008**, *130*, 13202-13203.

[41] Y. Li, Z. Li, C. Wang, H. Li, H. Lu, B. Xu, W. Tian, *J. Polym. Sci., Part A: Polym. Chem.* **2008***, 48,* 2765-2776.

[42] P. Bäuerle, F. Würthner, G. Götz, F. Effenberger, *Synthesis* **1993**, 1099-1103.

[43] J. Takagi, K. Sato, J. F. Hartwig, T. Ishiyama, N. Miyaura, *Tetrahedron Lett.* **2002**, *43*, 5649-5651.

[44] J. Hellberg, T. Remonen, F. Allared, J. Slätt, M. Svensson, *Synthesis* **2003**, *14*, 2199-2205.

[45] D. Mutaguchi, K. Okumoto, Y. Ohsedo, K. Moriwaki, Y. Shirota, *Org. Electron*. **2003**, *4*, 49-59.

[46] A. Jaafari, V. Ouzeau, M. Ely, F. Rodriguez, K. Chane-Ching, A. Yassar, J. J. Aaron, *Synth. Met.* **2004**, *147*, 183-189.

[47] J.-M. L'Helgoual'ch, G. Bentabed-Ababsa, F. Chevallier, M. Yonehara, M. Uchiyama, A. Derdour, F. Mongin, *Chem. Commun.* **2008**, 5375-5377.

[48] O. V. Dolomanov, L. J. Bourhis, R. J. Gildea, J. A. K. Howard, H. J. Puschmann, *J. Appl. Cryst.* **2009**, *42*, 339-341.

[49] L. Porrès, A. Holland, L.-O. Pålsson, A. P. Monkman, C. Kemp, A. Beeby, *J. Fluoresc.* **2006**, *16*, 267-272.

[50] M. A. Albota, C. Xu, W. W. Webb, *Appl. Opt.* **1998**, *37*, 7352-7356.

[51] a) Gaussian 03, Revision D.02, M. J. Frisch, G. W. Trucks, H. B. Schlegel, G. E. Scuseria, M. A. Robb, J. R. Cheeseman, J. A. Montgomery, Jr., T. Vreven, K. N. Kudin, J. C. Burant, J. M. Millam, S. S. Iyengar, J. Tomasi, V. Barone, B. Mennucci, M. Cossi, G. Scalmani, N. Rega, G. A. Petersson, H. Nakatsuji, M. Hada, M. Ehara, K. Toyota, R. Fukuda, J. Hasegawa, M. Ishida, T. Nakajima, Y. Honda, O. Kitao, H. Nakai, M. Klene, X. Li, J. E. Knox, H. P. Hratchian, J. B. Cross, V. Bakken, C. Adamo, J. Jaramillo, R. Gomperts, R. E. Stratmann, O. Yazyev, A. J. Austin, R. Cammi, C. Pomelli, J. W. Ochterski, P. Y. Ayala, K.

Morokuma, G. A. Voth, P. Salvador, J. J. Dannenberg, V. G. Zakrzewski, S. Dapprich, A. D. Daniels, M. C. Strain, O. Farkas, D. K. Malick, A. D. Rabuck, K. Raghavachari, J. B. Foresman, J. V. Ortiz, Q. Cui, A. G. Baboul, S. Clifford, J. Cioslowski, B. B. Stefanov, G. Liu, A. Liashenko, P. Piskorz, I. Komaromi, R. L. Martin, D. J. Fox, T. Keith, M. A. Al-Laham, C. Y. Peng, A. Nanayakkara, M. Challacombe, P. M. W. Gill, B. Johnson, W. Chen, M. W. Wong, C. Gonzalez, J. A. Pople, Gaussian, Inc., Wallingford CT, **2004**; b) Gaussian 09, Revision A.02, M. J. Frisch, G. W. Trucks, H. B. Schlegel, G. E. Scuseria, M. A. Robb, J. R. Cheeseman, G. Scalmani, V. Barone, B. Mennucci, G. A. Petersson, H. Nakatsuji, M. Caricato, X. Li, H. P. Hratchian, A. F. Izmaylov, J. Bloino, G. Zheng, J. L. Sonnenberg, M. Hada, M. Ehara, K. Toyota, R. Fukuda, J. Hasegawa, M. Ishida, T. Nakajima, Y. Honda, O. Kitao, H. Nakai, T. Vreven, J. A. Montgomery, Jr., J. E. Peralta, F. Ogliaro, M. Bearpark, J. J. Heyd, E. Brothers, K. N. Kudin, V. N. Staroverov, R. Kobayashi, J. Normand, K. Raghavachari, A. Rendell, J. C. Burant, S. S. Iyengar, J. Tomasi, M. Cossi, N. Rega, J. M. Millam, M. Klene, J. E. Knox, J. B. Cross, V. Bakken, C. Adamo, J. Jaramillo, R. Gomperts, R. E. Stratmann, O. Yazyev, A. J. Austin, R. Cammi, C. Pomelli, J. W. Ochterski, R. L. Martin, K. Morokuma, V. G. Zakrzewski, G. A. Voth, P. Salvador, J. J. Dannenberg, S. Dapprich, A. D. Daniels, Ö. Farkas, J. B. Foresman, J. V. Ortiz, J. Cioslowski, D. J. Fox, Gaussian, Inc., Wallingford CT, **2009**.

[52] S. Tretiak, V. Chernyak, *J. Chem. Phys.* **2003**, *119*, 8809-8823.

[53] D. Jacquemin, A. Planchat, C. Adamo, B. Mennucci, *J. Chem. Theory Comput.* **2012**, *8*, 2359-2372.

[54] A. Kokalj, *J. Mol. Graph. Model.* **1999**, *17*, 176-179.

Entry for the Table of Contents
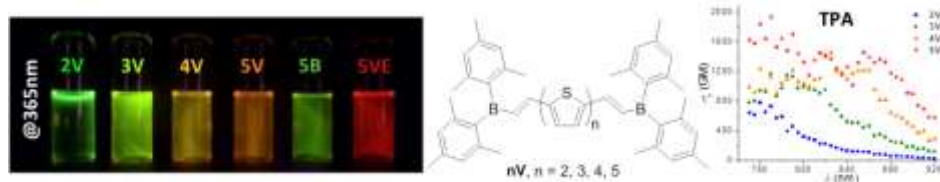
Oligothiophene based quadrupolar chromophores with BMes$_2$ terminal groups have been synthesized in high isolated yields. These compounds have large two-photon absorption (TPA) cross-sections in the NIR region. Experimental results show that the TPA cross-section increases with increasing length of the bridge. DFT and TD-DFT calculations complement the experimental findings and contribute to their interpretation.

▌ **Fluorescence**

L. Ji, R. M. Edkins, L. J. Sewell, A. Beeby, A. S. Batsanov, K. Fucke, M. Drafz, J. A. K. Howard, O. Moutounet, F. Ibersiene, A. Boucekkine, E. Furet, Z. Liu, J.-F. Halet,* C. Katan,* T. B. Marder*

Experimental and theoretical studies of quadrupolar oligothiophene-cored chromophores containing dimesitylboryl moieties as π-accepting end-groups: Syntheses, structures, fluorescence, one- and two-photon absorption